



**University of Brasília - UnB**

Institute of Exact Sciences  
Department of Computer Science

# Towards Complete 3D Indoor Scene Understanding from a Single Point-of-View

Qualifying examination of the Ph.D. Program in Computer Science

**Aloisio Dourado Neto**

Supervisor  
Prof. Dr. Teófilo Emídio de Campos

Comitee

Prof. Dr. Anderson de Rezende Rocha  
Unicamp

Prof. Dr. Ricardo de Queiroz  
CIC/UnB

# Presentation Outline

- Introduction
  - Motivation
  - Problem statement
  - Objectives
- Research steps
- Work plan

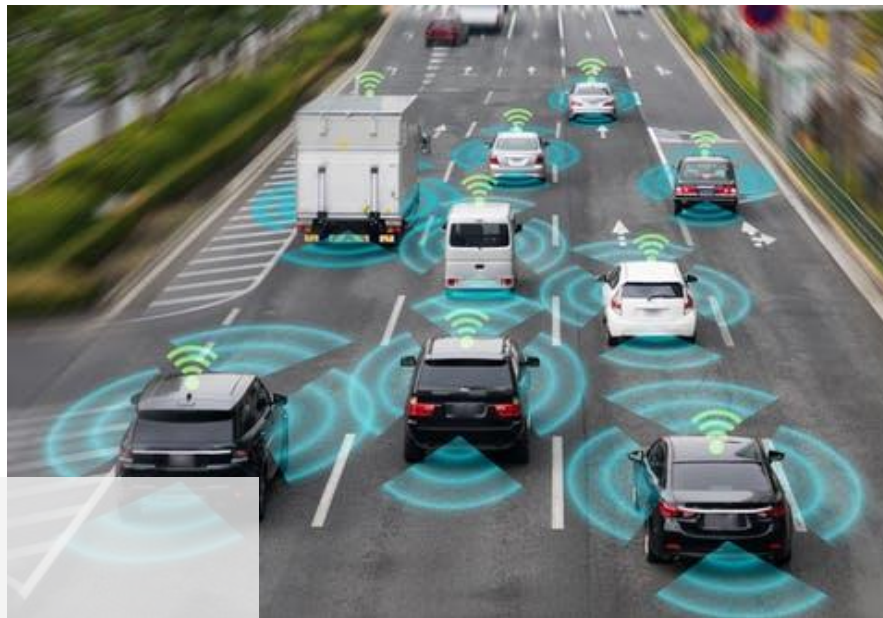
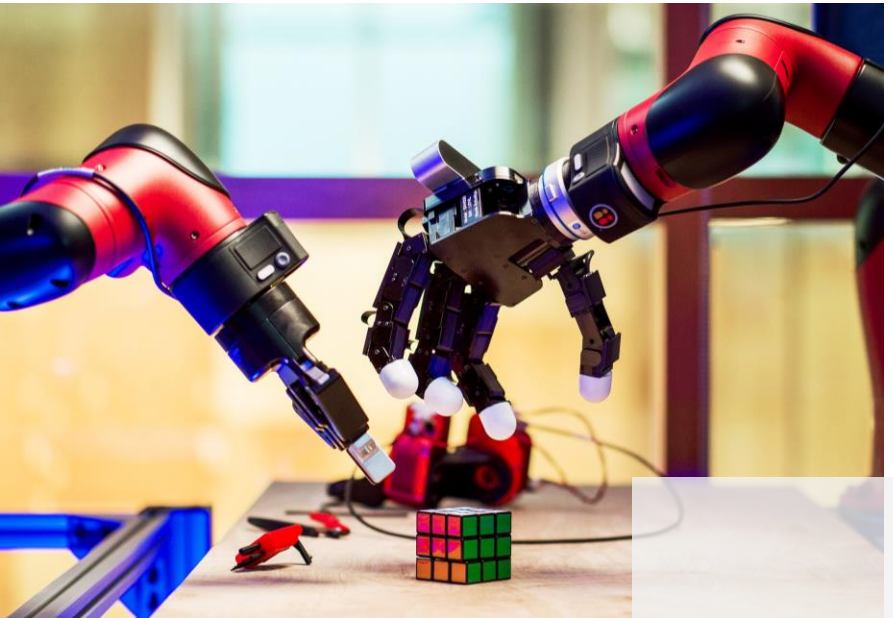
# Chapter 1

## Introduction



3D Scene  
Reasoning

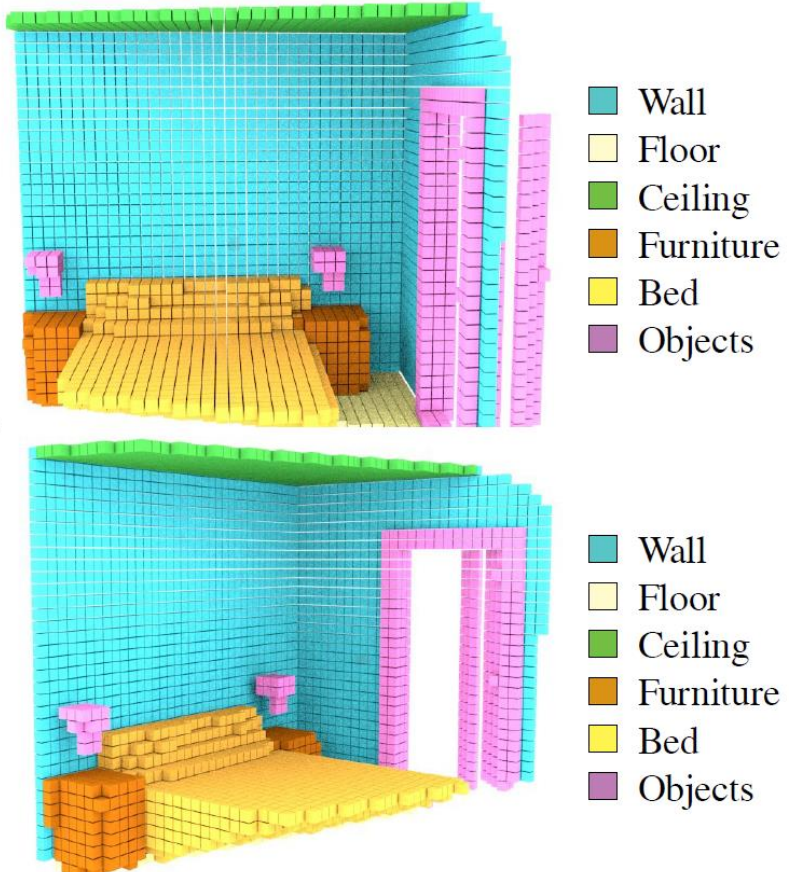
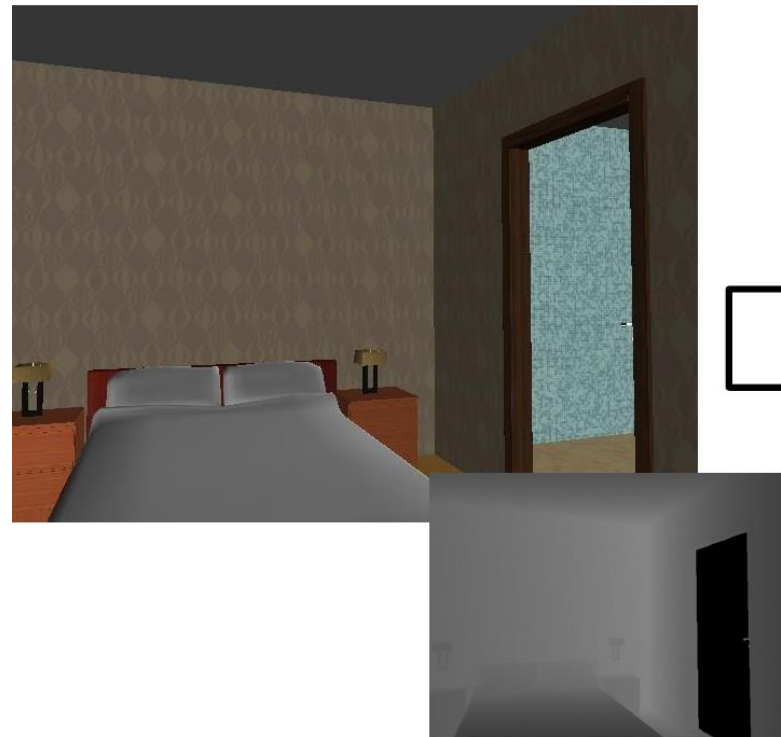




## Applications



# Semantic Scene Completion

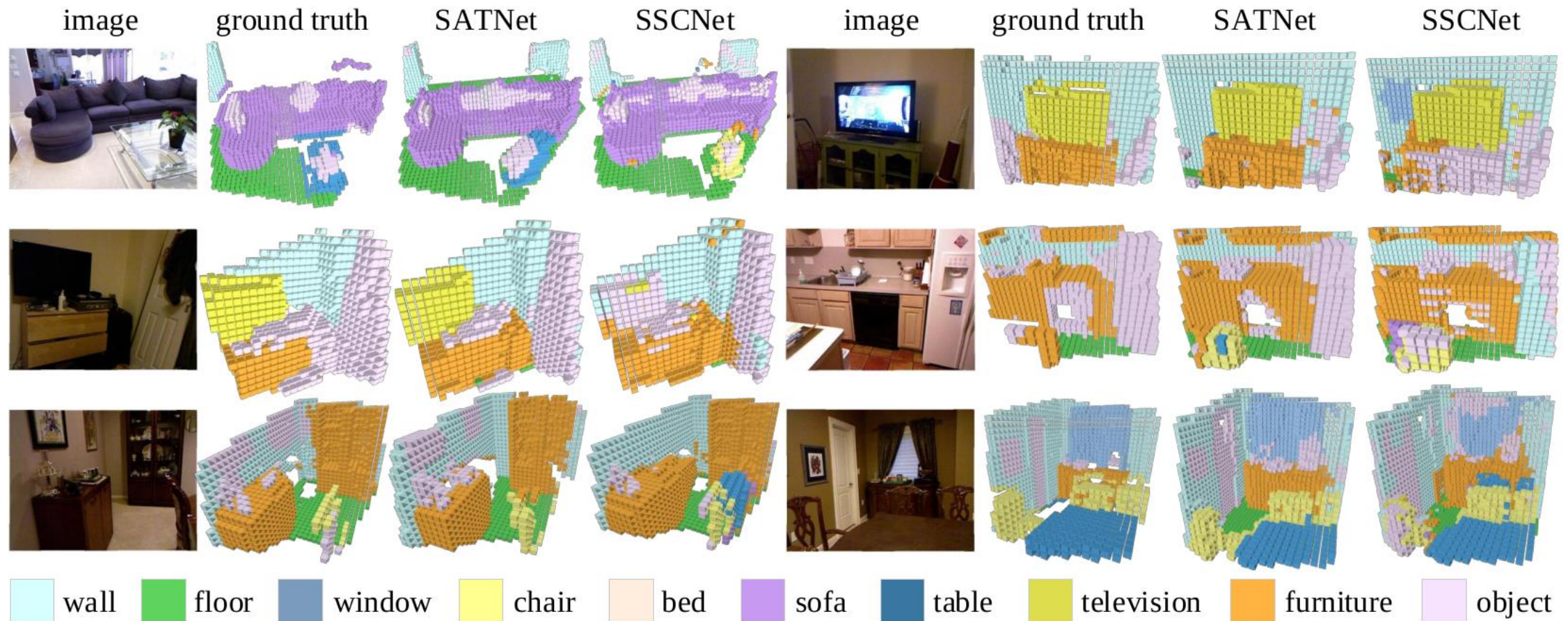


Introduced by Song *et al.*[107]  
in 2017

Trained a 3D CNN that jointly  
deals with both completion  
and semantic segmentation

[107] Song, S., Yu, F., Zeng, A., Chang, A.X., Savva, M., and Funkhouser, T.: Semantic Scene Completion from a Single Depth Image. In Proceedings of IEEE Conference on Computer Vision and Pattern Recognition (CVPR), Honolulu, Hawaii, July 21-26, pp. 190–198, Piscataway, NJ, July 2017. IEEE. 2, 3, 4, 18, 45, 46, 47, 51, 52, 53, 64, 68, 70

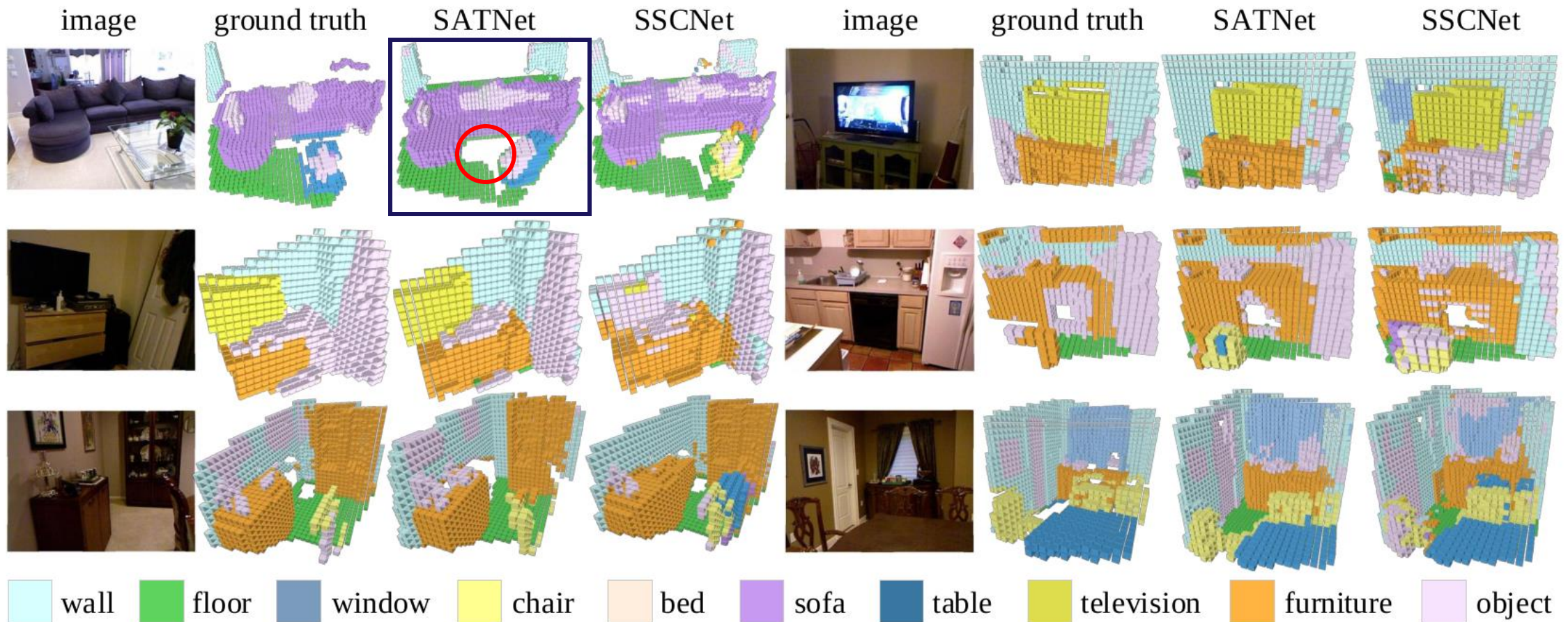
# Problem Statement



Qualitative results on NYUv2 dataset from Liu *et al.* [70]

[70] Liu, S., HU, Y., Zeng, Y., Tang, Q., Jin, B., Han, Y., and Li, X.: See and think: Disentangling semantic scene completion. In Bengio, S., Wallach, H., Larochelle, H., Grauman, K., Cesa-Bianchi, N., and Garnett, R. (eds.): Proceedings of Conference on Neural Information Processing Systems 31 (NIPS), pp. 263–274, Reed Hook, NY, 2018. Curran Associates, Inc.  
<http://papers.nips.cc/paper/7310-see-and-think-disentangling-semantic-scene-completion.pdf>. 2, 4, 45, 47, 52, 53, 58, 59

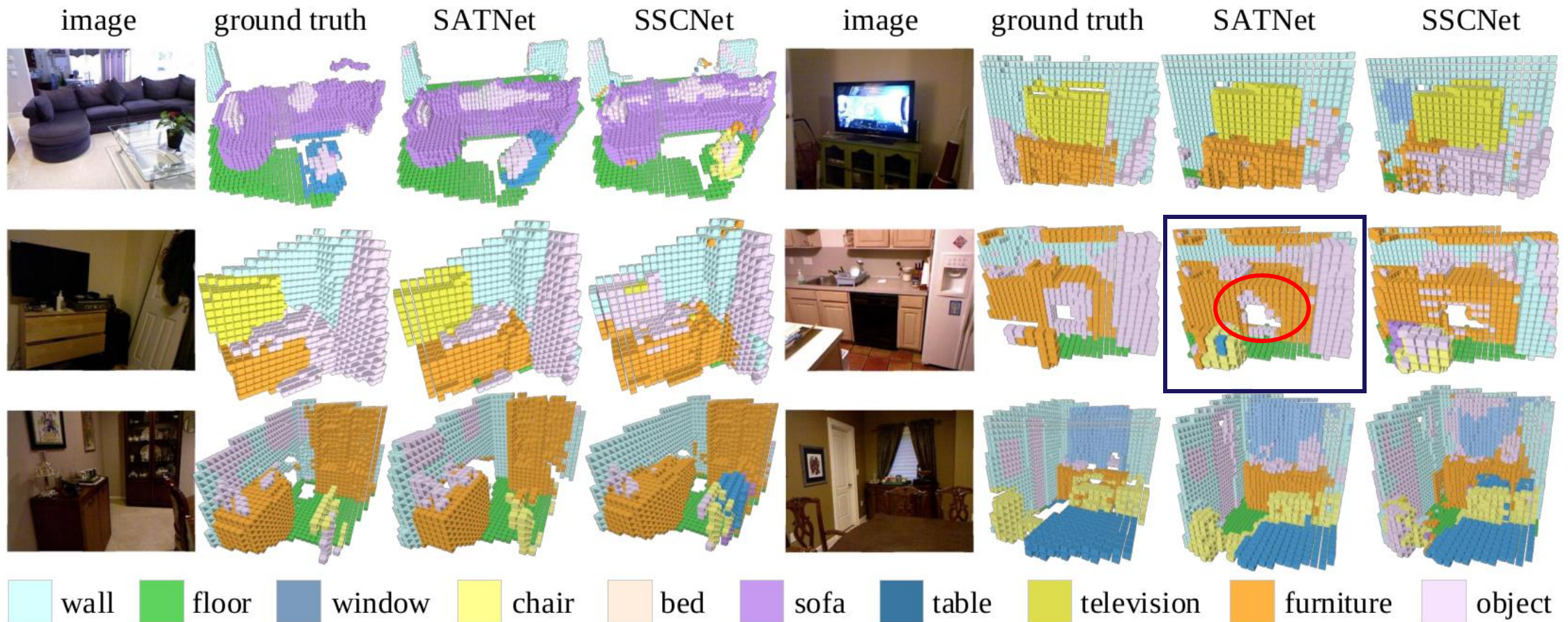
# Problem Statement



Qualitative results on NYUv2 dataset from Liu *et al.* [70]

[70] Liu, S., HU, Y., Zeng, Y., Tang, Q., Jin, B., Han, Y., and Li, X.: See and think: Disentangling semantic scene completion. In Bengio, S., Wallach, H., Larochelle, H., Grauman, K., Cesa-Bianchi, N., and Garnett, R. (eds.): Proceedings of Conference on Neural Information Processing Systems 31 (NIPS), pp. 263–274, Reed Hook, NY, 2018. Curran Associates, Inc.  
<http://papers.nips.cc/paper/7310-see-and-think-disentangling-semantic-scene-completion.2,4,45,47,52,53,58,59>

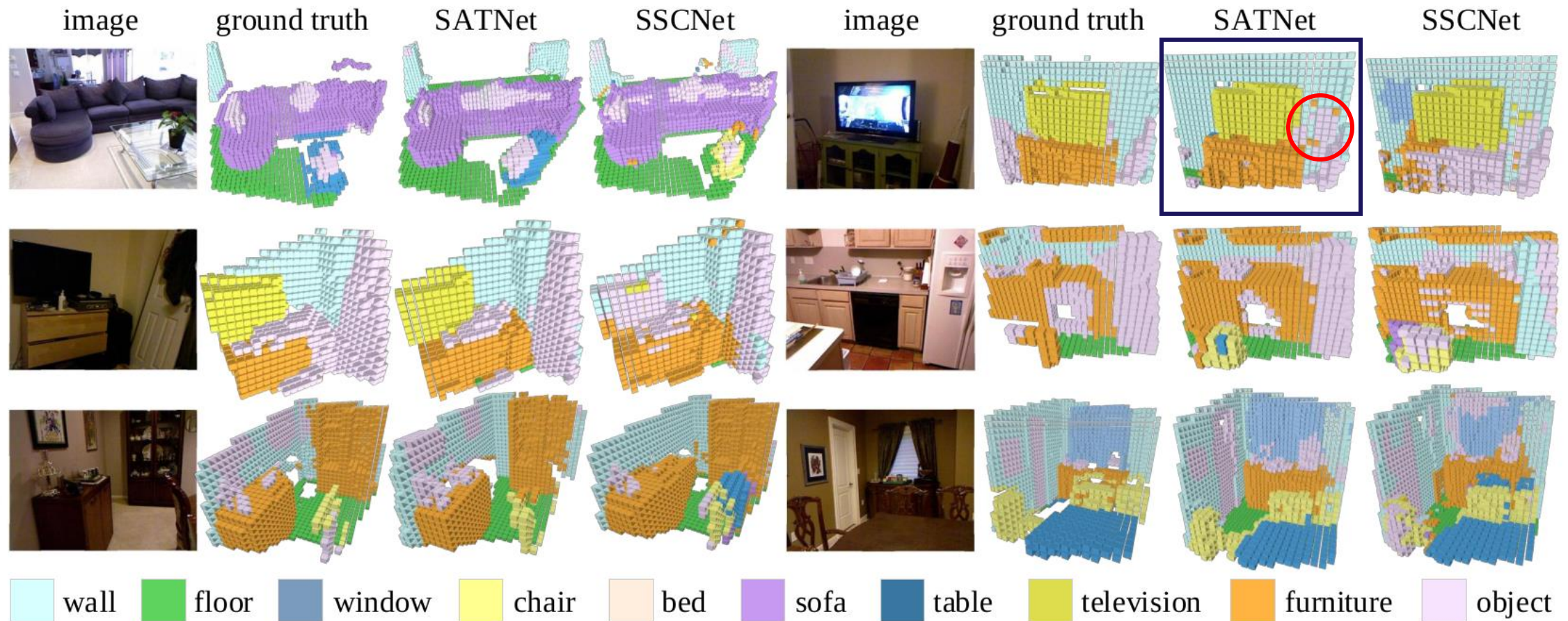
# Problem Statement



Qualitative results on NYUv2 dataset from Liu *et al.* [70]

[70] Liu, S., HU, Y., Zeng, Y., Tang, Q., Jin, B., Han, Y., and Li, X.: See and think: Disentangling semantic scene completion. In Bengio, S., Wallach, H., Larochelle, H., Grauman, K., Cesa-Bianchi, N., and Garnett, R. (eds.): Proceedings of Conference on Neural Information Processing Systems 31 (NIPS), pp. 263–274, Reed Hook, NY, 2018. Curran Associates, Inc.  
<http://papers.nips.cc/paper/7310-see-and-think-disentangling-semantic-scene-completion.pdf>. 2, 4, 45, 47, 52, 53, 58, 59

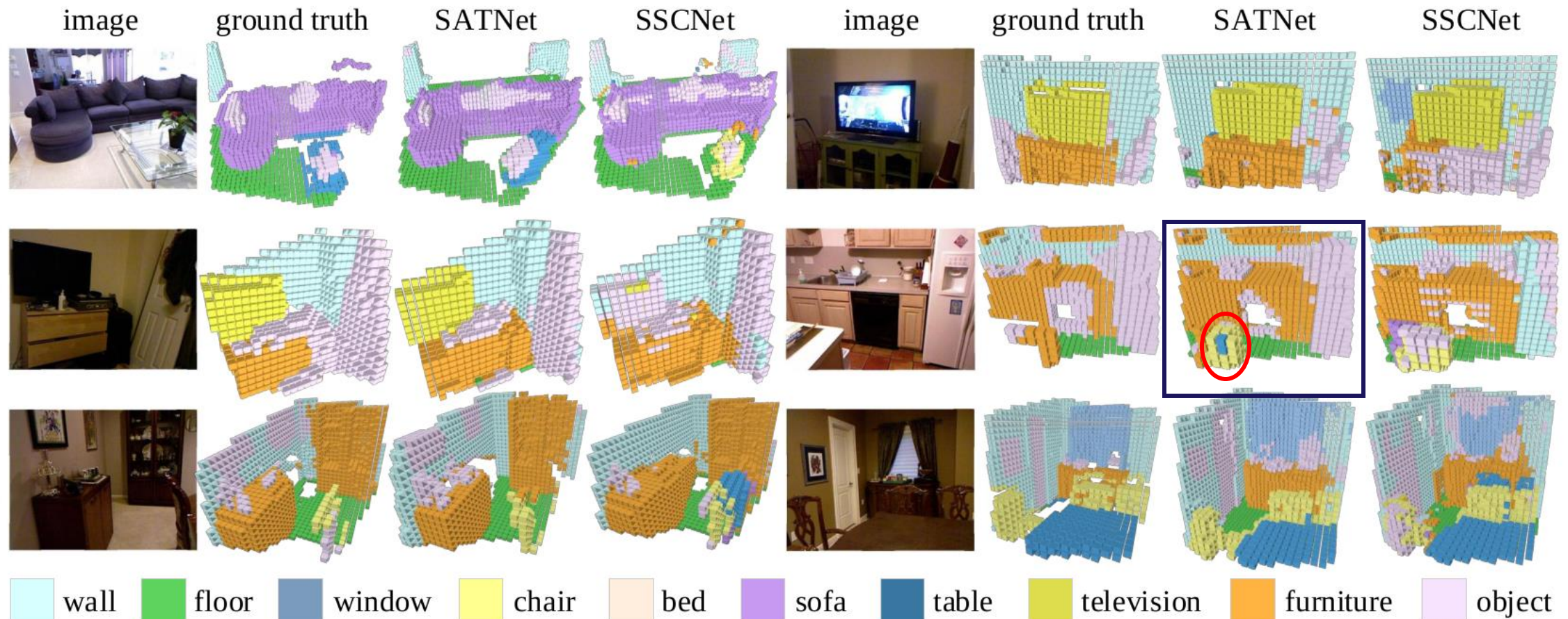
# Problem Statement



Qualitative results on NYUv2 dataset from Liu *et al.* [70]

[70] Liu, S., HU, Y., Zeng, Y., Tang, Q., Jin, B., Han, Y., and Li, X.: See and think: Disentangling semantic scene completion. In Bengio, S., Wallach, H., Larochelle, H., Grauman, K., Cesa-Bianchi, N., and Garnett, R. (eds.): Proceedings of Conference on Neural Information Processing Systems 31 (NIPS), pp. 263–274, Reed Hook, NY, 2018. Curran Associates, Inc.  
<http://papers.nips.cc/paper/7310-see-and-think-disentangling-semantic-scene-completion.pdf>. 2, 4, 45, 47, 52, 53, 58, 59

# Problem Statement



Qualitative results on NYUv2 dataset from Liu *et al.* [70]

[70] Liu, S., HU, Y., Zeng, Y., Tang, Q., Jin, B., Han, Y., and Li, X.: See and think: Disentangling semantic scene completion. In Bengio, S., Wallach, H., Larochelle, H., Grauman, K., Cesa-Bianchi, N., and Garnett, R. (eds.): Proceedings of Conference on Neural Information Processing Systems 31 (NIPS), pp. 263–274, Reed Hook, NY, 2018. Curran Associates, Inc.  
<http://papers.nips.cc/paper/7310-see-and-think-disentangling-semantic-scene-completion.pdf>. 2, 4, 45, 47, 52, 53, 58, 59

## Problem Statement

- Two main deficiencies of current approaches:
  - the RGB part of the RGB-D image is not completely explored;
  - they are limited to the restricted FOV of depth sensors like Kinect

# Objectives

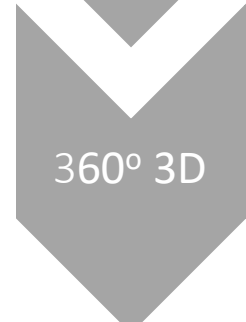
New tools and models that could push SSC solutions towards a complete understanding of the whole indoor scene



- to assess the benefits of domain adaptation techniques in the context of image segmentation



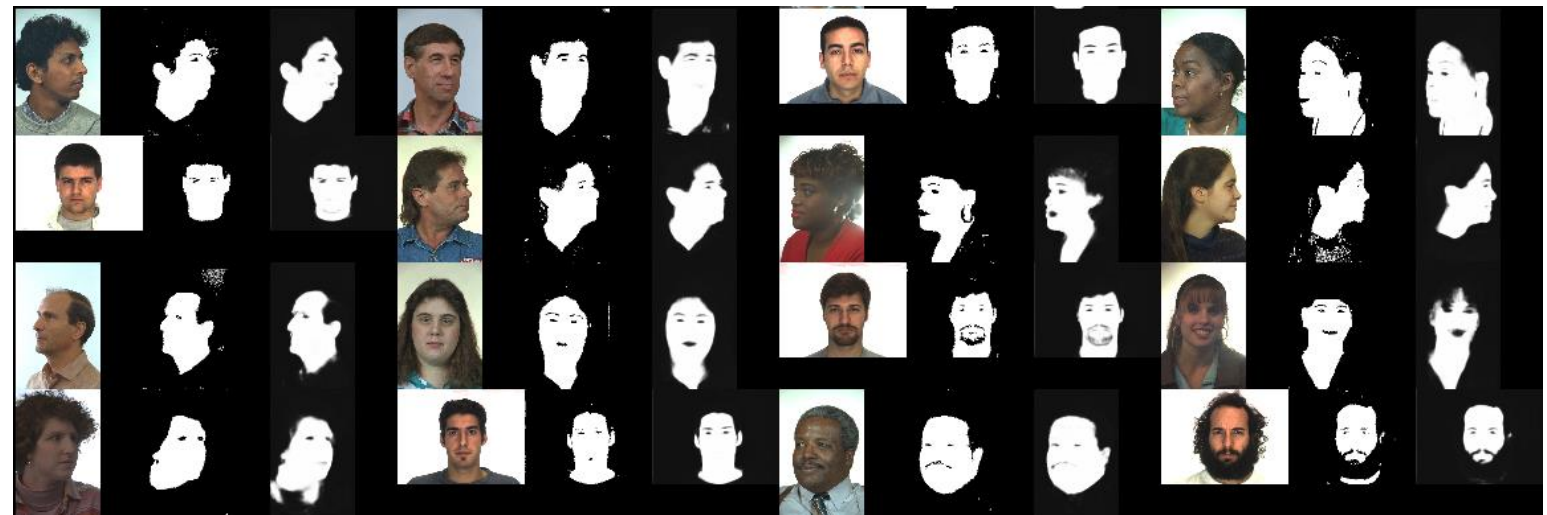
- to propose and evaluate a new SSC model that uses the RGB information present in RGB-D images



- to propose and evaluate a solution to perform 360° SSC

# Chapter 3

## Fully Convolutional Networks, Domain Adaptation and Semantic Segmentation



# Fully Convolutional Networks, Domain Adaptation and Semantic Segmentation

## Why work on 2D?

- Work on 3D is hard
- Less previous works to compare!
- Start to explore domain adaptation and segmentation in an easier domain

[53] Kakumanu, P., Makrogiannis, S., and Bourbakis, N.: A survey of skin-color modeling and detection methods. *Pattern Recognition*, 40(3):1106 – 1122, 2007, ISSN 0031-3203.27

[12] Brancati, N., Pietro, G.D., Frucci, M., and Gallo, L.: Human skin detection through correlation rules between the YCb and YCr subspaces based on dynamic color clustering. *Computer Vision and Image Understanding*, 155:33 – 42, 2017, ISSN 1077-3142.  
27, 28, 35, 36, 39, 42

# Fully Convolutional Networks, Domain Adaptation and Semantic Segmentation

- Why the skin segmentation application?
  - Research field where some criticisms regarding the use of CNNs/FCNs are made:
    - the need for large training datasets [53]
    - the specificity or lack of generalization of neural nets
    - long prediction time [12]
  - We wanted to try to refute those criticisms

[53] Kakumanu, P., Makrogiannis, S., and Bourbakis, N.: A survey of skin-color modeling and detection methods. *Pattern Recognition*, 40(3):1106 – 1122, 2007, ISSN 0031-3203.27

[12] Brancati, N., Pietro, G.D., Frucci, M., and Gallo, L.: Human skin detection through correlation rules between the YCb and YCr subspaces based on dynamic color clustering. *Computer Vision and Image Understanding*, 155:33 – 42, 2017, ISSN 1077-3142.  
27, 28, 35, 36, 39, 42

## Previous Works

Historically, color-based or texture methods were preferred [49, 100]

Current state-of-the-art works still rely on local approaches:

- Skin-color separation [12, 33]
- Patch-based CNN [74]

The use of domain adaptation methods for this problem is not common

[12] Brancati, N., Pietro, G.D., Frucci, M., and Gallo, L.: Human skin detection through correlation rules between the YCb and YCr subspaces based on dynamic color clustering. *Computer Vision and Image Understanding*, 155:33 – 42, 2017, ISSN 1077-3142.  
27, 28, 35, 36, 39, 42

[33] Faria, R.A.D. and Hirata Jr., R.: Combined correlation rules to detect skin based on dynamic color clustering. In *Proceedings of the 13th International Joint Conference on Computer Vision, Imaging and Computer Graphics Theory and Applications (VISAPP)*, vol. 5, pp. 309–316. INSTICC, SciTePress, 2018, ISBN 978-989-758-290-5. 28, 35, 36

[49] Huynh-Thu, Q., Meguro, M., and Kaneko, M.: Skin-Color-Based Image Segmentation and Its Application in Face Detection. In *MVA*, pp. 48–51, 2002. 27, 39

[74] Lumini, A. and Nanni, L.: Fair comparison of skin detection approaches on publicly available datasets. *Techn. rep.*, Cornell University Library, CoRR/cs.CV, August 2019. arXiv:1802.02531 (v3). 28, 43

[100] Shrivastava, V.K., Londhe, N.D., Sonawane, R.S., and Suri, J.S.: Computer-aided diagnosis of psoriasis skin images with HOS, texture and color features. *Comput. Methods Prog. Biomed.*, 126(C):98–109, Apr. 2016, ISSN 0169-2607. 27

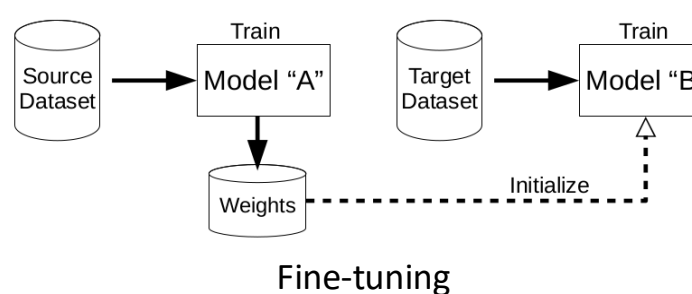
# Experiments

## In-domain:

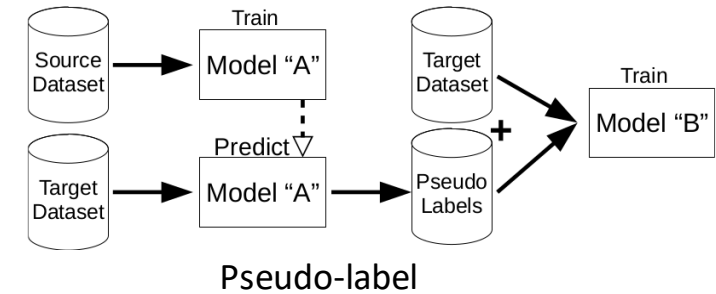
- Local CNN vs Holistic FCN
- Comparison to current color-based state-of-the-art

## Cross-domain:

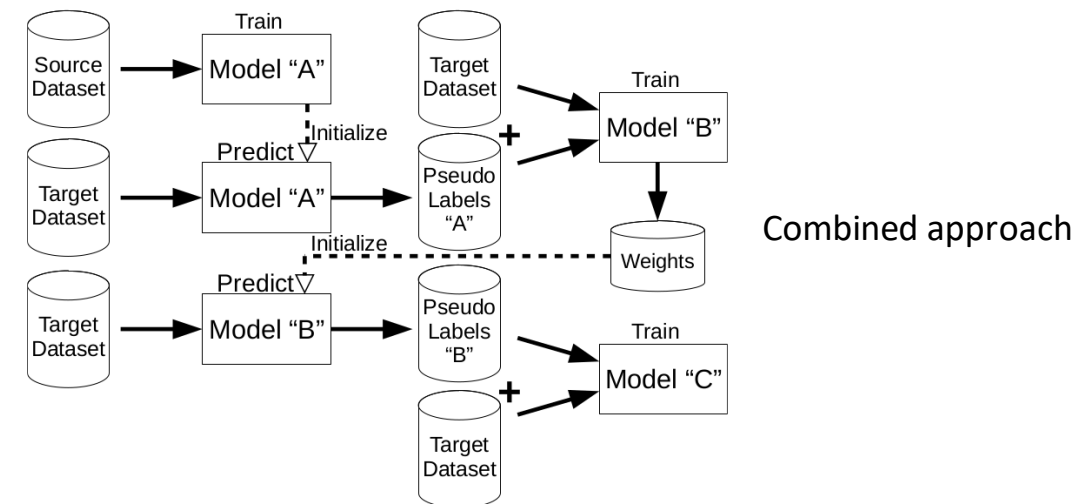
- Assessment of 3 simple methods



Fine-tuning



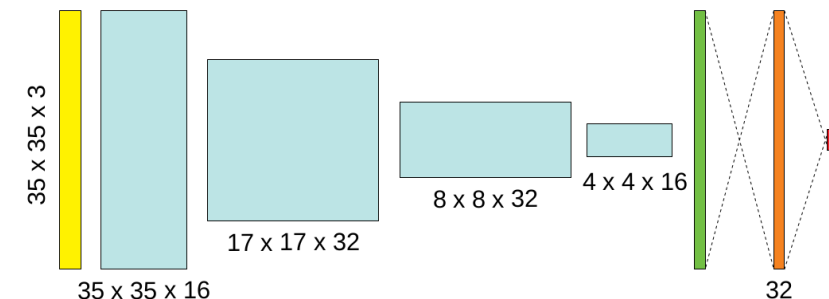
Pseudo-label



Combined approach

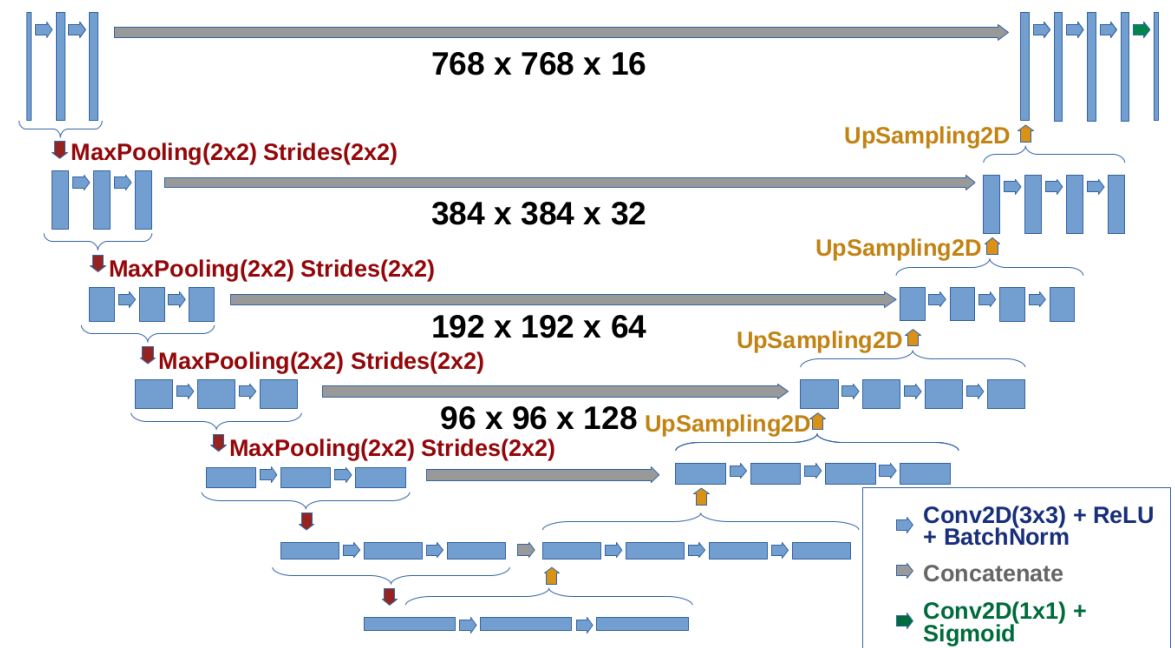
# Models

## Local, Patch-based CNN



- Input
- 2D Convolution( $3 \times 3$ ) + ReLu + MaxPooling
- Flatten
- Dense
- Dense + Sigmoid

## Holistic, u-shaped FCN



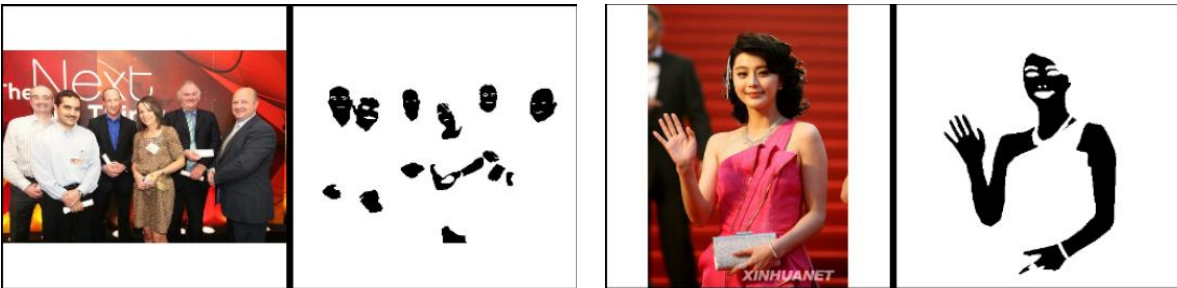
- Conv2D( $3 \times 3$ ) + ReLU + BatchNorm
- Concatenate
- Conv2D( $1 \times 1$ ) + Sigmoid

# Datasets

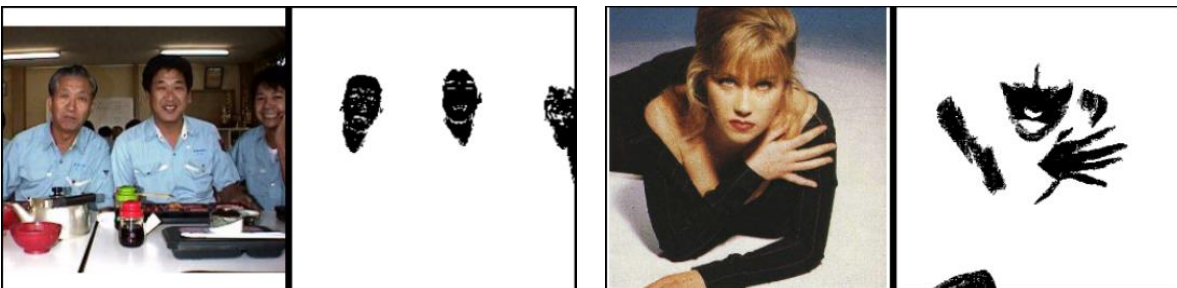
SFA[15]  
(1,118 images)



Pratheepan[117]  
(78 images)



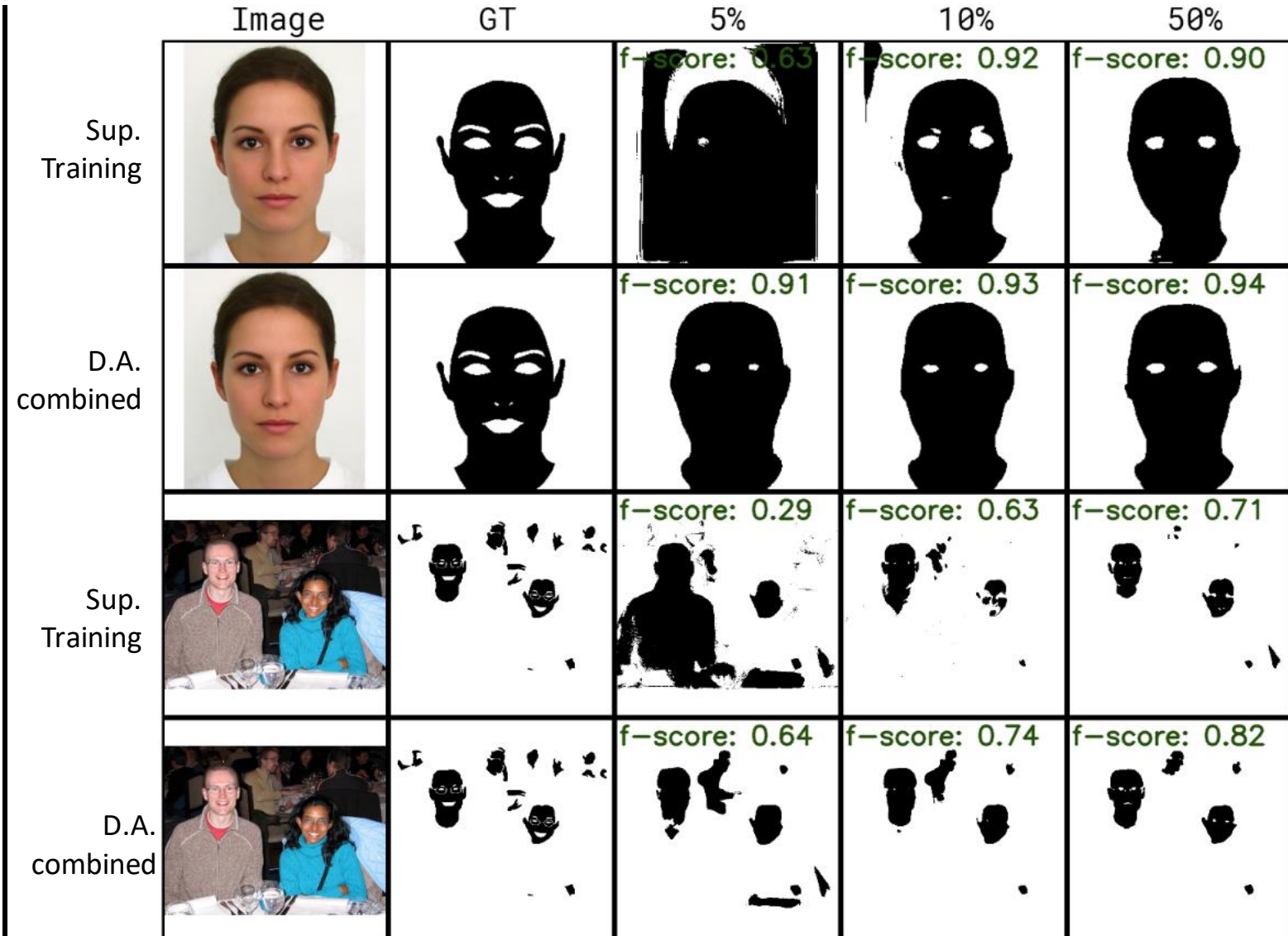
Compaq[51]  
(4,670 images)



VPU[93]  
(290 images)



# Supervised Training VS Domain Adaptation



Comparison of source only vs. domain adaptation combined approach in the Compaq→Pratheepan scenario

# Conclusions

Refuted criticisms regarding  
the use of Deep Convolu-  
tional Networks for skin  
segmentation

- Color or texture separation may suffice:
  - Our two CNN approaches performed much better than the color-based state-of-the-art
- CNNs are slow:
  - Our U-Net inference time was enough for real-time applications
- CNNs need too much data to generalize:
  - With no labeled data -> 60% improvement

# Publication

## ***Domain Adaptation for Holistic Skin Detection***

**Domain Adaptation for Holistic Skin Detection**

Aloisio Dourado  
Department of Computer Science, University of Brasilia  
Brasilia, DF, 70910-900, Brazil  
[aloisio.dourado.bh@gmail.com](mailto:aloisio.dourado.bh@gmail.com)

Frederico Guth  
[fredguth@fredguth.com](mailto:fredguth@fredguth.com)

Teófilo de Campos  
[t.decampos@oxfordalumni.org](mailto:t.decampos@oxfordalumni.org)  
<http://cic.unb.br/~teodecampos/>

Li Weigang  
[weigang@unb.br](mailto:weigang@unb.br)  
<http://cic.unb.br/~weigang/>

Human skin detection in images is a widely studied topic of Computer Vision for which it is commonly accepted that analysis of pixel color or local patches may suffice. This is because skin regions appear to be relatively uniform and many argue that there is a small chromatic variation among different samples. However, we found that there are strong biases in the datasets commonly used to train or tune skin detection methods. Furthermore, the lack of contextual information may hinder the performance of local approaches. In this paper we present a comprehensive evaluation of holistic and local Convolutional Neural Network (CNN) approaches on in-domain and cross-domain experiments and compare with state-of-the-art pixel-based approaches. We also propose a combination of inductive transfer learning and unsupervised domain adaptation methods, which are evaluated on different domains under several amounts of labelled data availability. We show a clear superiority of CNN over pixel-based approaches even without labelled training samples on the target domain. Furthermore, we provide experimental support for the counter-intuitive superiority of holistic over local approaches for human skin detection.

*Keywords:* Domain Adaptation, Skin segmentation, CNN.

**1. Introduction**

Human skin detection is the task of identifying which pixels of an image correspond to skin. The segmentation of skin regions in images has several applications: video surveillance, people tracking, human computer interaction, face detection and recognition and gesture detection, among many others.<sup>[2][3]</sup>

Before the boom of Convolutional Neural Networks (CNNs), most approaches

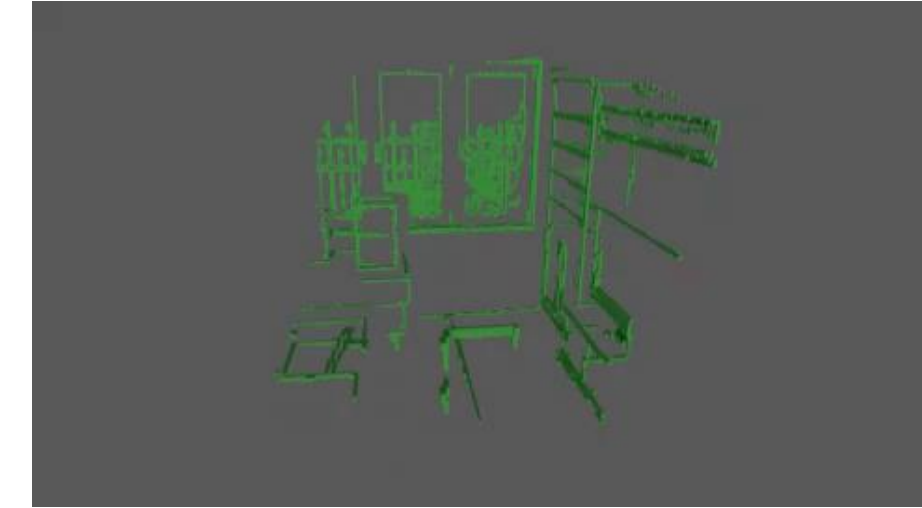
1

\*Submitted to International Journal of Pattern Recognition and Artificial Intelligence (Capes Qualis B1)

[30] Dourado, A., Guth, F., de Campos, T.E., and Weigang, L.: Domain adaptation for holistic skin detection. Tech. Rep. arXiv:1903.0969, Cornell University Library, 2019. <http://arxiv.org/abs/1903.0969>. 6, 26

# Chapter 4

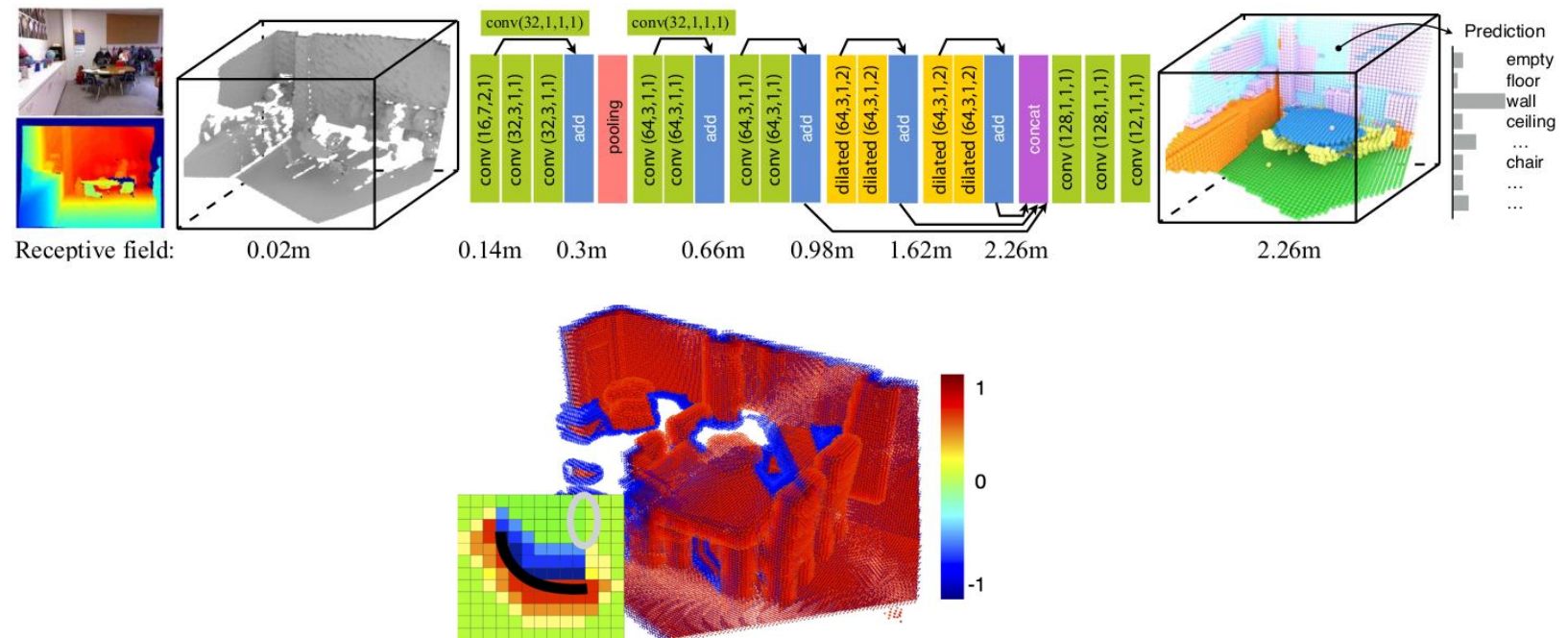
Using RGB Edges to  
improve Semantic  
Scene Completion  
from RGB-D Images



# Previous Works

## Depth maps only

- **SSCNET: Song et al. [107]**
  - Seminal paper
  - Proposed F-TSDF encoding
  - Introduced SUNCG Dataset

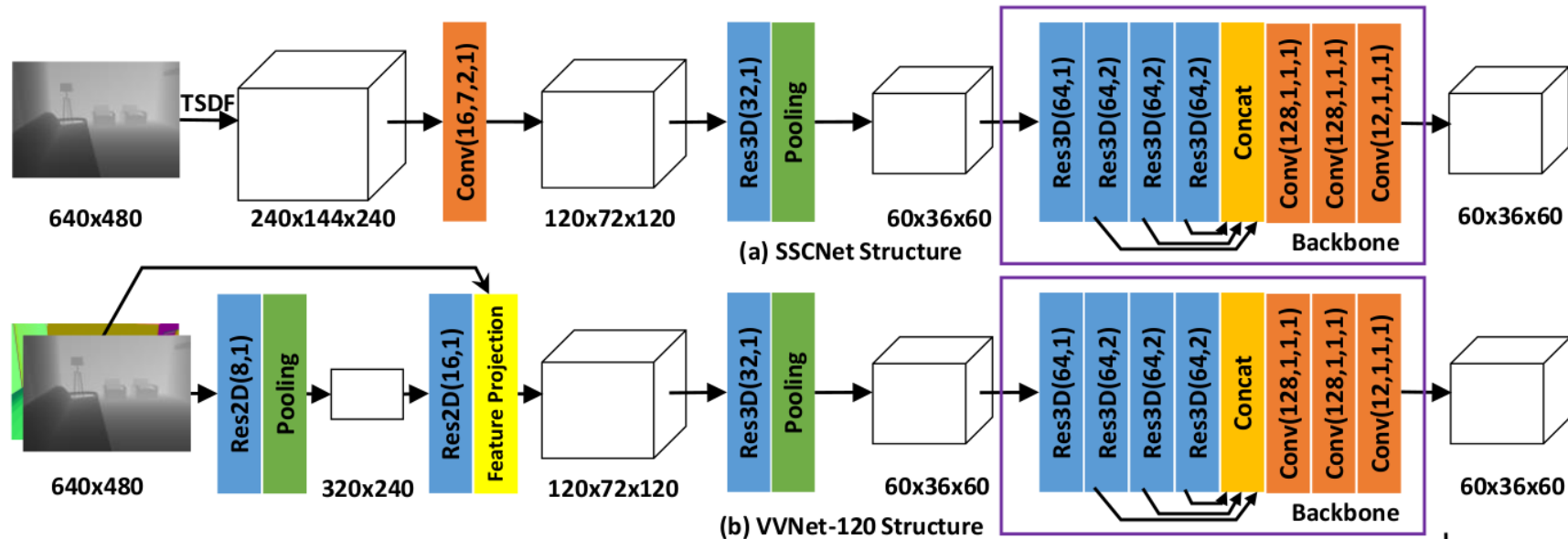


[107] Song, S., Yu, F., Zeng, A., Chang, A.X., Savva, M., and Funkhouser, T.: Semantic Scene Completion from a Single Depth Image. In Proceedings of IEEE Conference on Computer Vision and Pattern Recognition (CVPR), Honolulu, Hawaii, July 21–26, pp. 190–198, Piscataway, NJ, July 2017. IEEE. 2, 3, 4, 18, 45, 46, 47, 51, 52, 53, 64, 68, 70

# Previous Works

Depth maps only

- Guo and Tong [40]:
  - 2D features projected to 3D



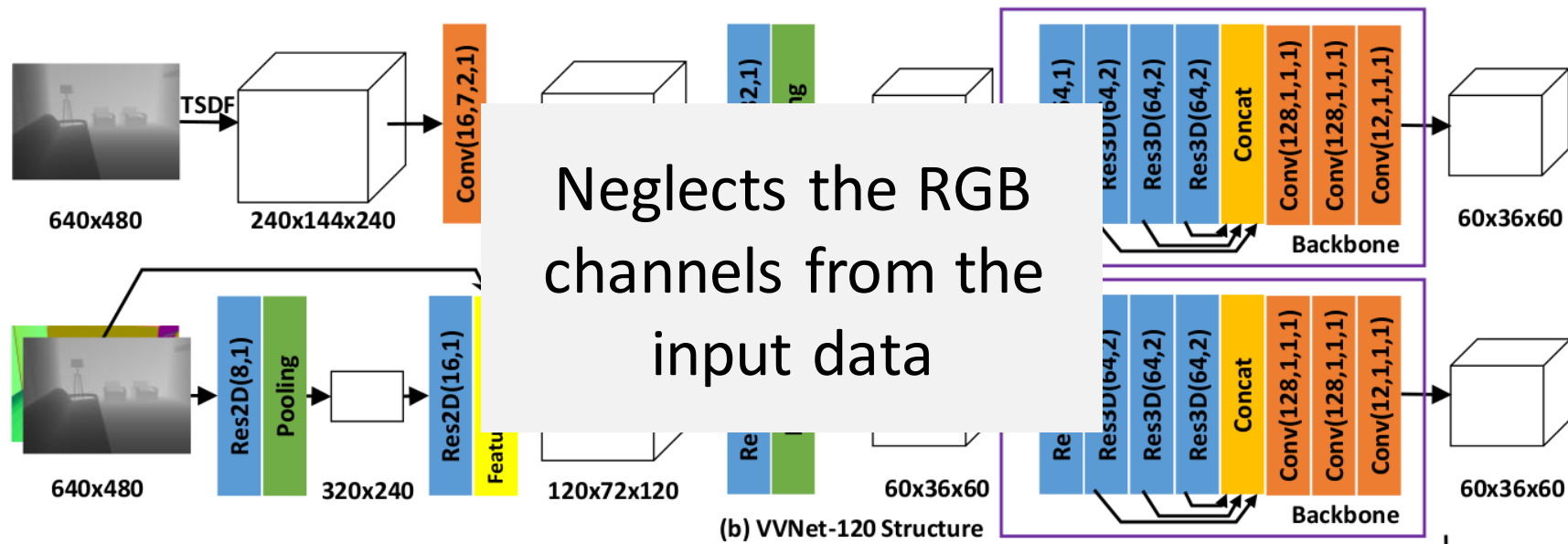
[40] Guo, Y. and Tong, X.: View-Volume Network for Semantic Scene Completion from a Single Depth Image. In Proceedings of the Twenty-Seventh International Joint Conference on Artificial Intelligence, pp. 726–732, Stockholm, Sweden, July 2018. International Joint Conferences on Artificial Intelligence Organization, ISBN 978-0-9992411-2-7.

<https://doi.org/10.24963/ijcai.2018/101>. 2, 4, 18, 46, 52, 53

# Previous Works

Depth maps only

- Guo and Tong [40]:
  - 2D features projected to 3D



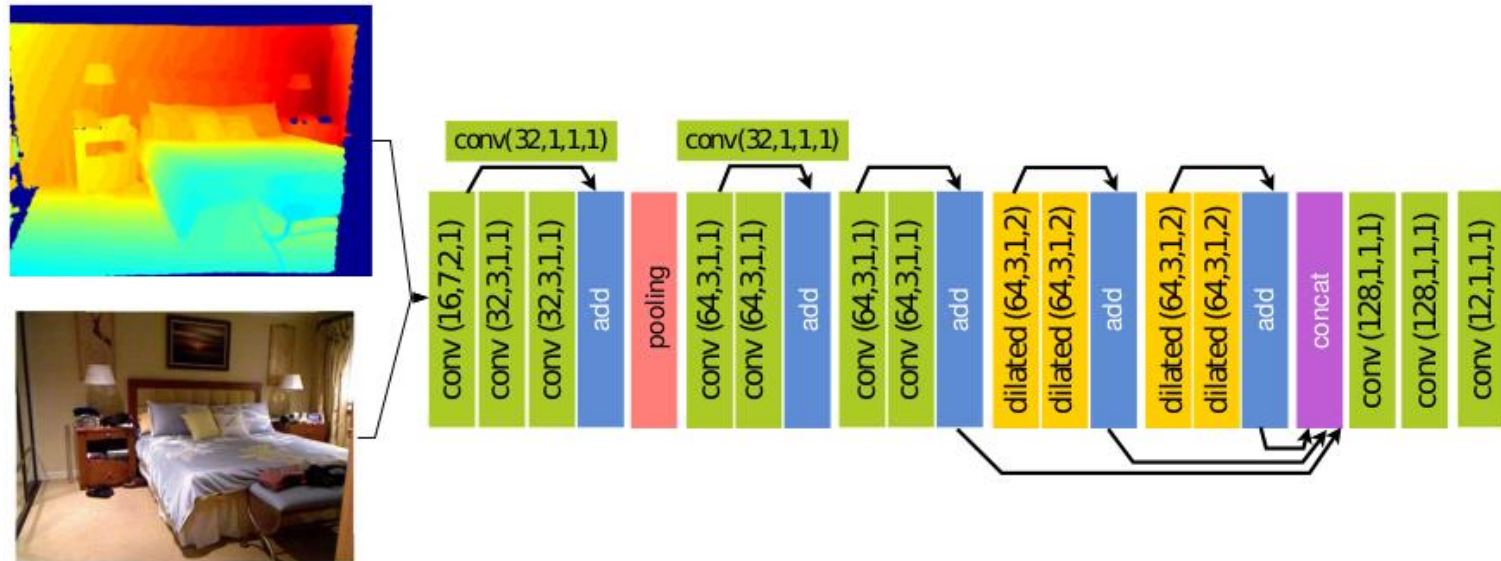
[40] Guo, Y. and Tong, X.: View-Volume Network for Semantic Scene Completion from a Single Depth Image. In Proceedings of the Twenty-Seventh International Joint Conference on Artificial Intelligence, pp. 726–732, Stockholm, Sweden, July 2018. International Joint Conferences on Artificial Intelligence Organization, ISBN 978-0-9992411-2-7.

<https://doi.org/10.24963/ijcai.2018/101>. 2, 4, 18, 46, 52, 53

# Previous Works

## Depth maps plus RGB

- Guedes *et al.*[38]

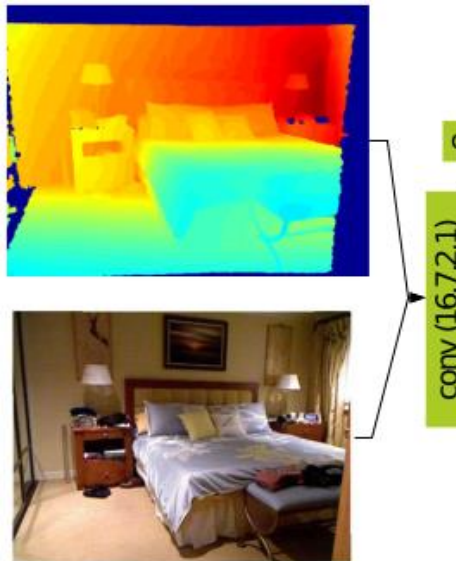


[38] Guedes, A.B.S., de Campos, T.E., and Hilton, A.: Semantic scene completion combining colour and depth: preliminary experiments. In ICCV workshop on 3D Reconstruction Meets Semantics (3DRMS), Venice, Italy, October 2017.  
Event webpage: <http://trimbot2020.webhosting.rug.nl/events/events-2017/3drms/>. Also published at arXiv:1802.04735. 4, 45, 46, 47, 52, 53

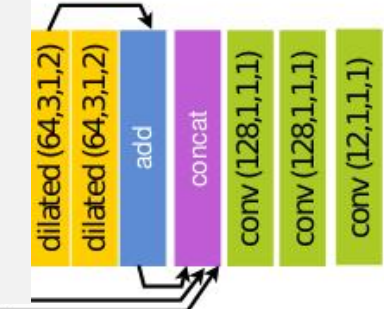
## Previous Works

Depth maps plus RGB

- Guedes *et al.*[38]



Suffers from RGB  
data sparsity after  
projection to 3D

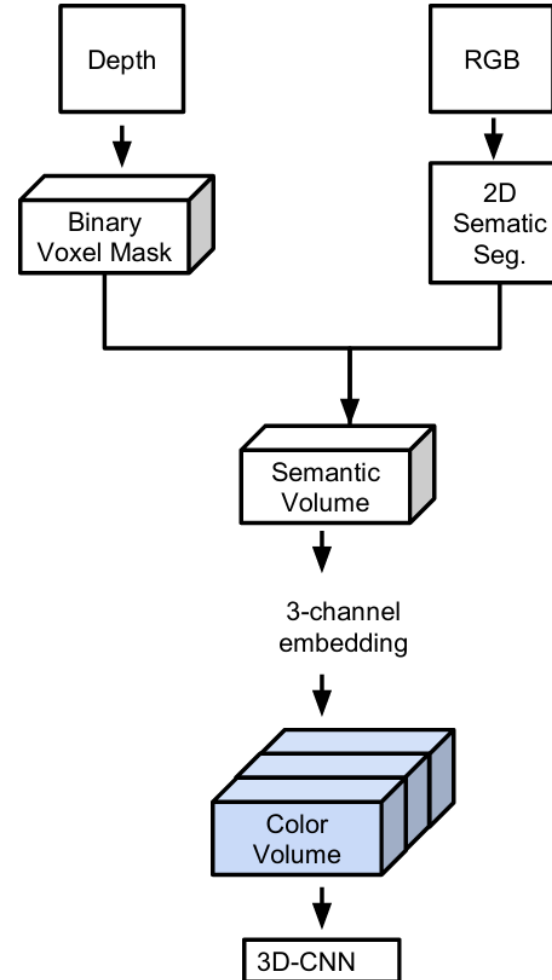


[38] Guedes, A.B.S., de Campos, T.E., and Hilton, A.: Semantic scene completion combining colour and depth: preliminary experiments. In ICCV workshop on 3D Reconstruction Meets Semantics (3DRMS), Venice, Italy, October 2017. Event webpage: <http://trimbot2020.webhosting.rug.nl/events/events-2017/3drms/>. Also published at arXiv:1802.04735. 4, 45, 46, 47, 52, 53

# Previous Works

## Depth map plus 2D segmentation

- Two stream 3D semantic scene completion: Garbade *et al.*[36]

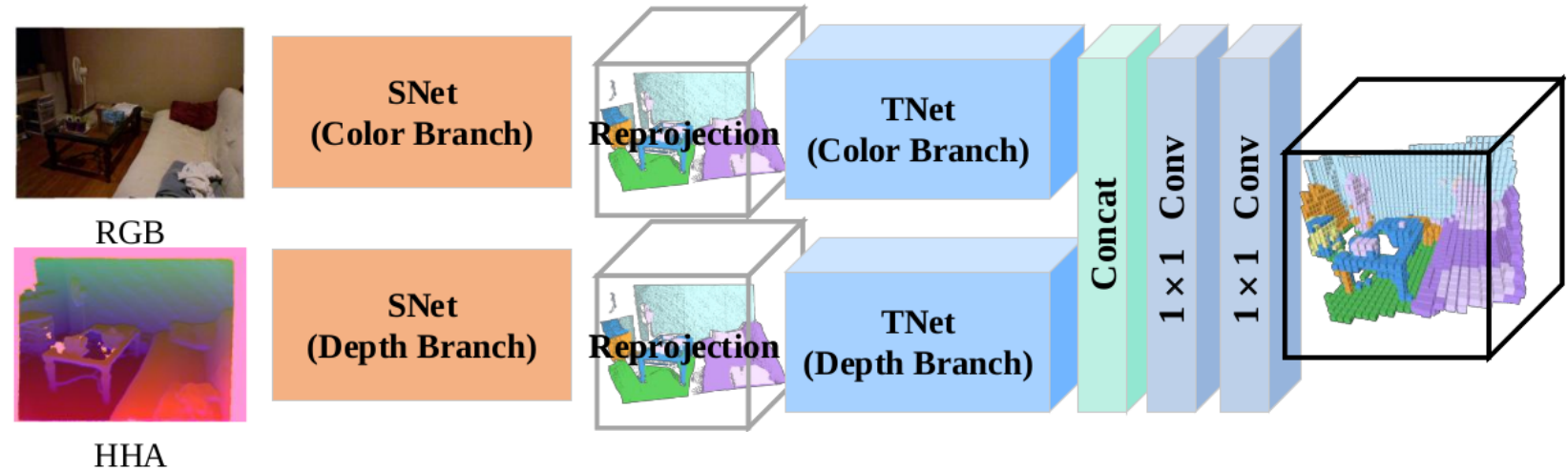


[36] Garbade, M., Sawatzky, J., Richard, A., and Gall, J.: Two stream 3D semantic scene completion. Tech. Rep. arXiv:1804.03550, Cornell University Library, 2018. <http://arxiv.org/abs/1804.03550>. 4, 45, 47, 52, 53

# Previous Works

Depth map plus 2D segmentation

- TNetFusion: Liu *et al.*[70]

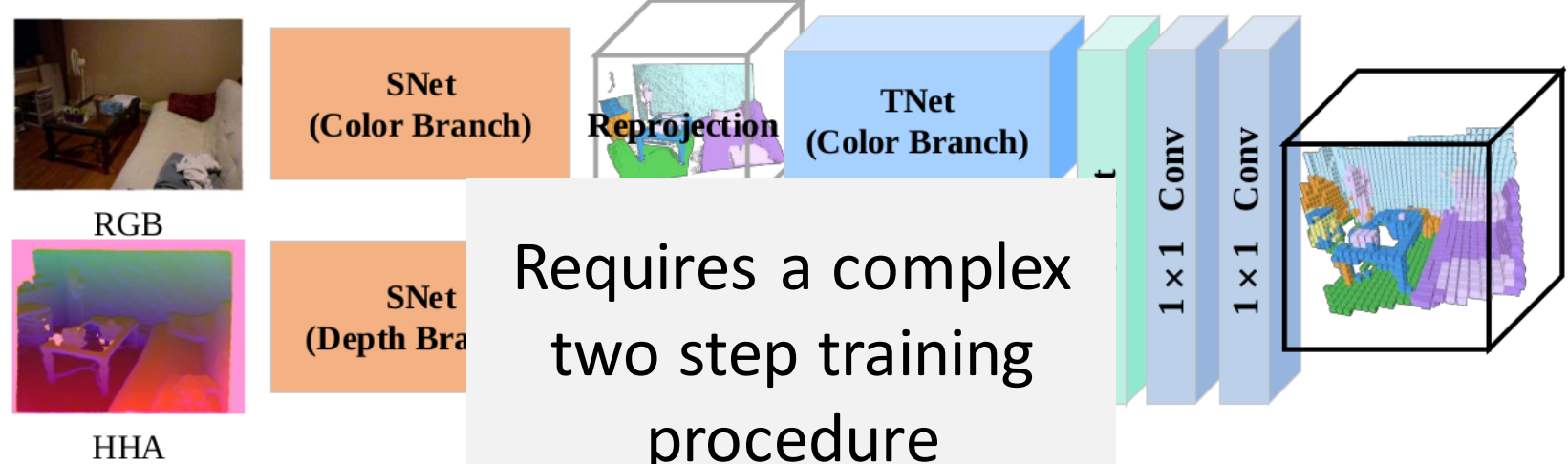


[70] Liu, S., HU, Y., Zeng, Y., Tang, Q., Jin, B., Han, Y., and Li, X.: See and think: Disentangling semantic scene completion. In Bengio, S., Wallach, H., Larochelle, H., Grauman, K., Cesa-Bianchi, N., and Garnett, R. (eds.): Proceedings of Conference on Neural Information Processing Systems 31 (NIPS), pp. 263–274, Reed Hook, NY, 2018. Curran Associates, Inc.  
<http://papers.nips.cc/paper/7310-see-and-think-disentangling-semantic-scene-completion.pdf>. 2, 4, 45, 47, 52, 53, 58, 59

## Previous Works

Depth map plus 2D segmentation

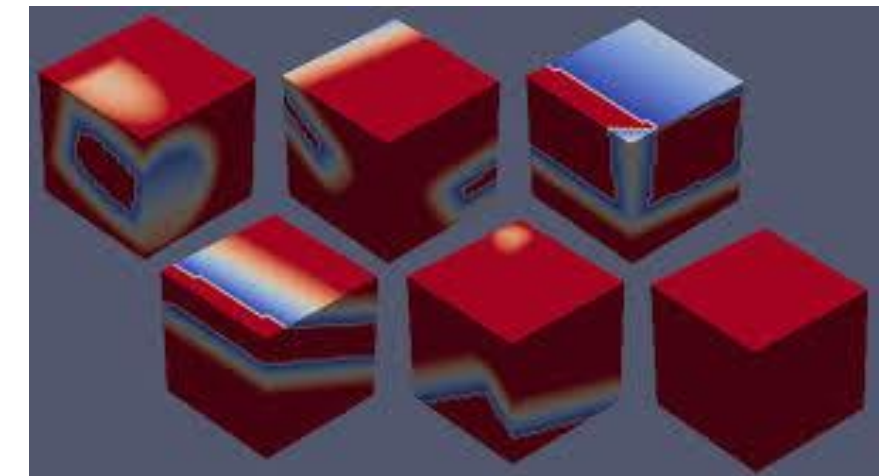
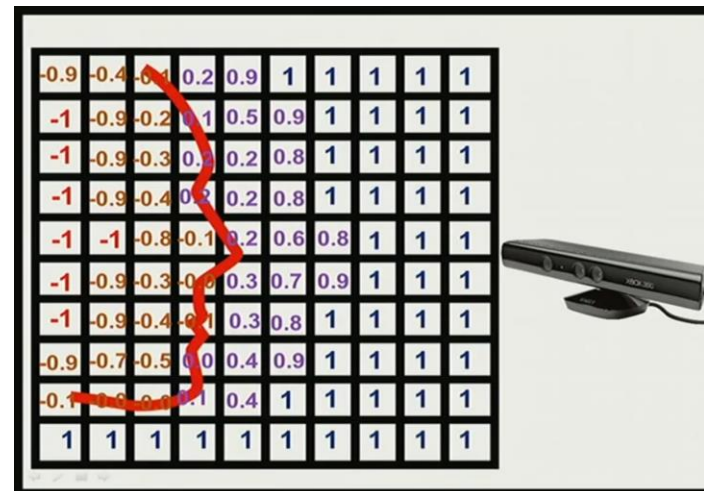
- TNetFusion: Liu *et al.*[70]



[70] Liu, S., HU, Y., Zeng, Y., Tang, Q., Jin, B., Han, Y., and Li, X.: See and think: Disentangling semantic scene completion. In Bengio, S., Wallach, H., Larochelle, H., Grauman, K., Cesa-Bianchi, N., and Garnett, R. (eds.): Proceedings of Conference on Neural Information Processing Systems 31 (NIPS), pp. 263–274, Reed Hook, NY, 2018. Curran Associates, Inc.  
<http://papers.nips.cc/paper/7310-see-and-think-disentangling-semantic-scene-completion.pdf>. 2, 4, 45, 47, 52, 53, 58, 59

# TSDF VS F-TSDF

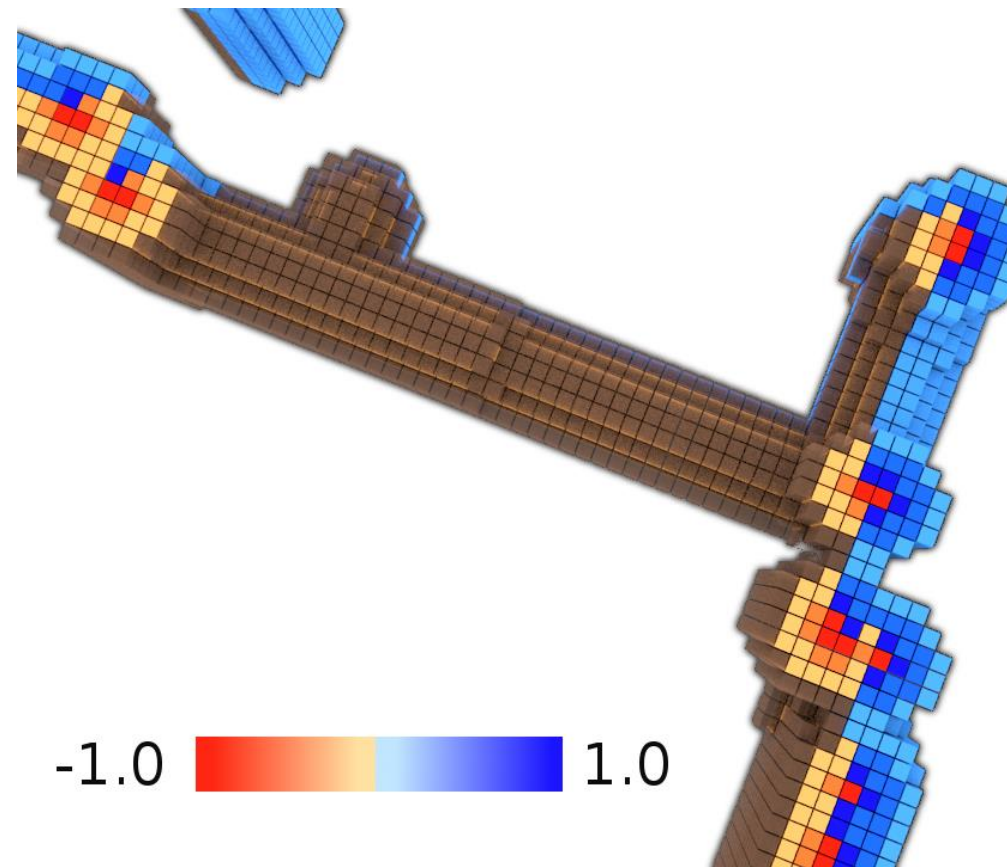
- TSDF: Truncated Signed Distance Function



TSDF

TSDF  
VS  
F-TSDF

- F-TSDF: Flipped Truncated Signed Distance Function

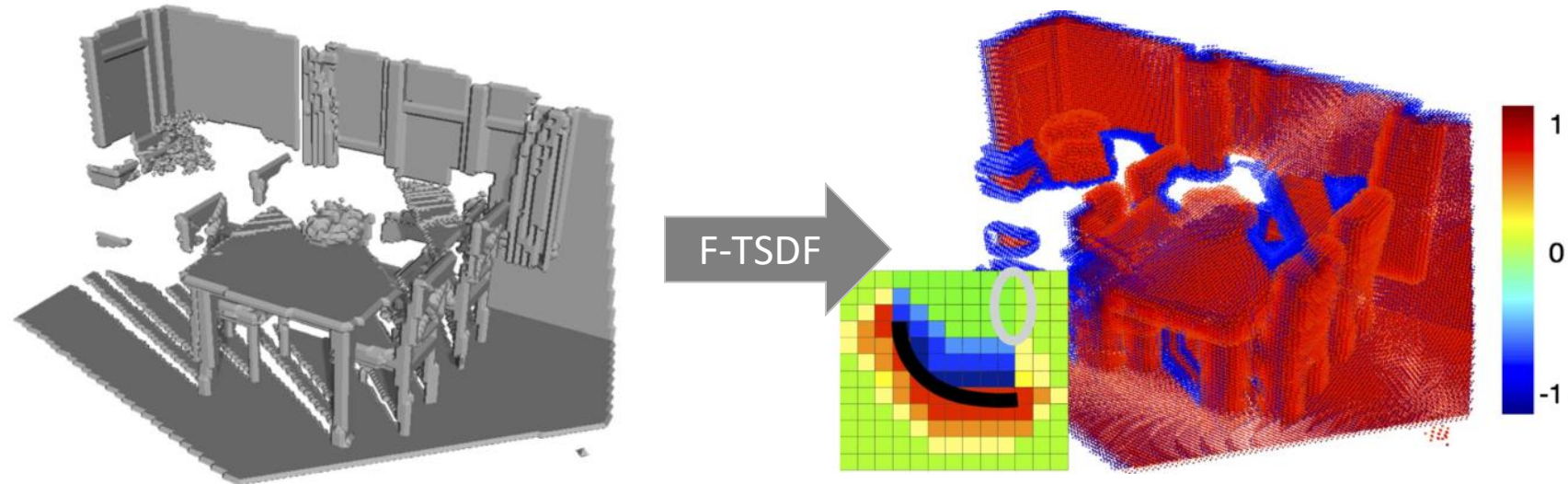


F-TSDF

$$\text{F-TSDF} = \text{sign}(\text{TSDF}) \cdot (1 - |\text{TSDF}|)$$

## F-TSDF and the RGB Volume

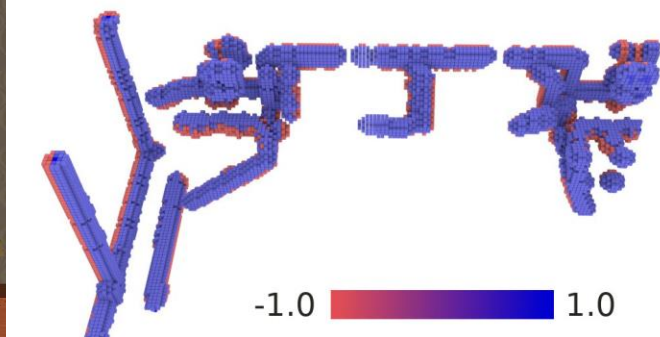
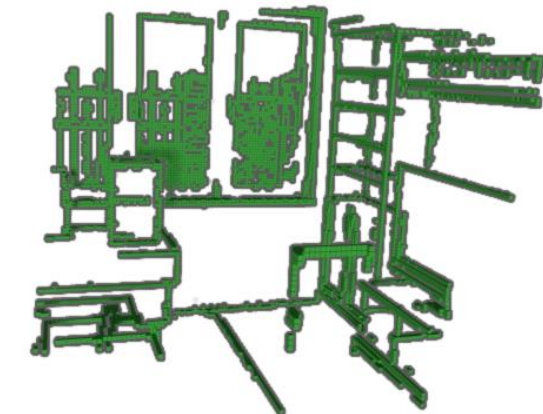
- It is possible to apply F-TSDF to the occupancy volume



- However, RGB data is not binary!

# Our Approach: EdgeNet

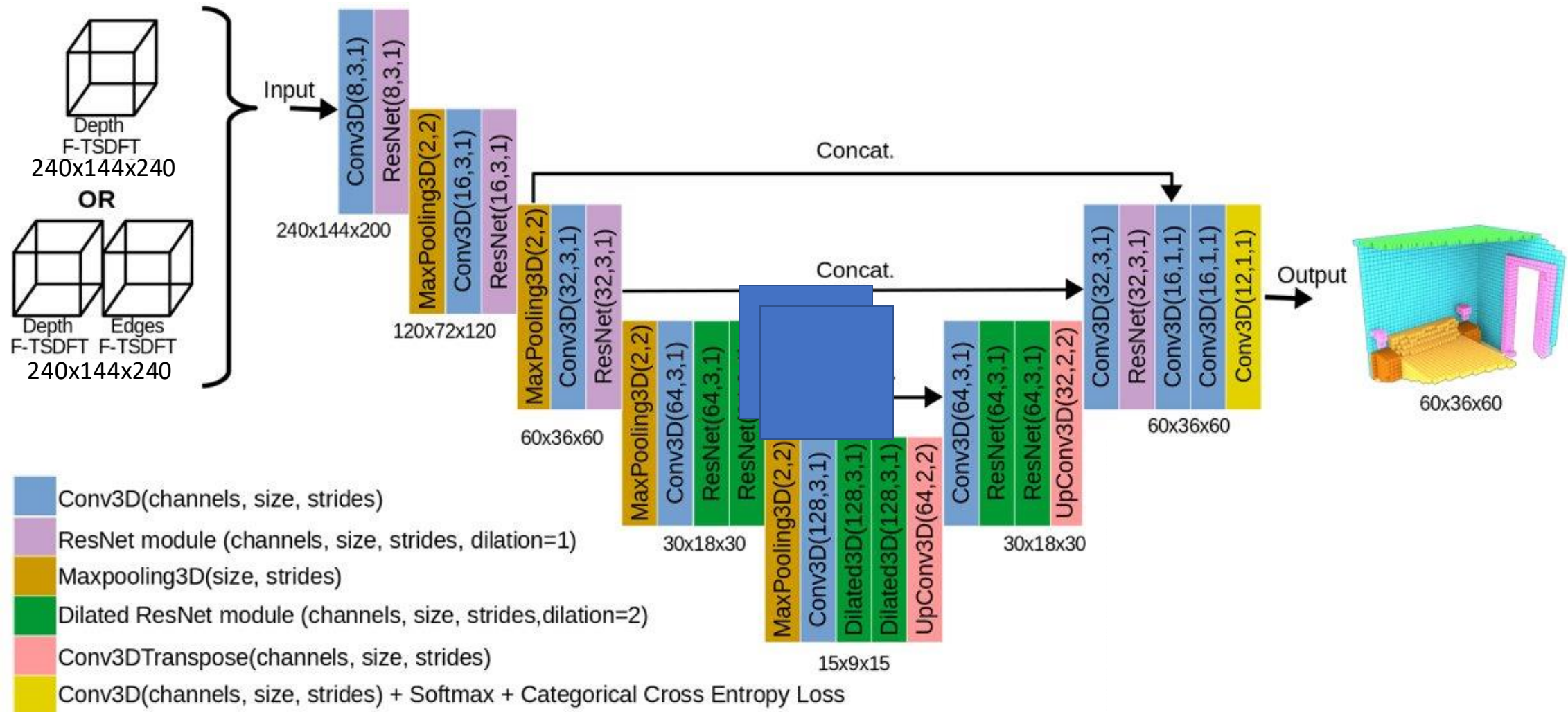
- We extract information from RGB data using Canny Edge detector before F-TSDF



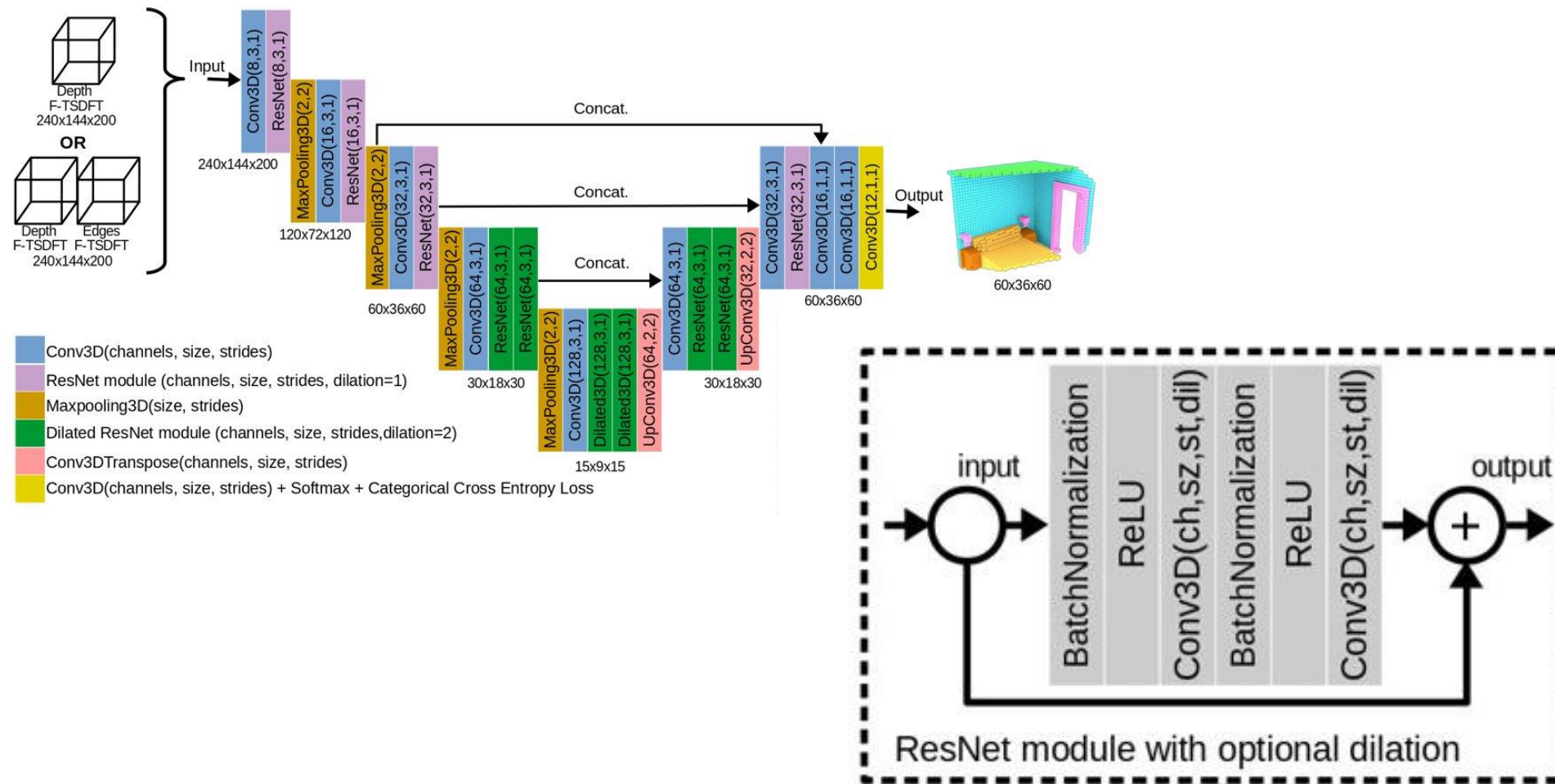
## Our implementation

- Offline F-TSDF calculation using portable C++ CUDA code
- We provide a software interface between CUDA and Python
- Preprocessing code is independent from the deep learning framework

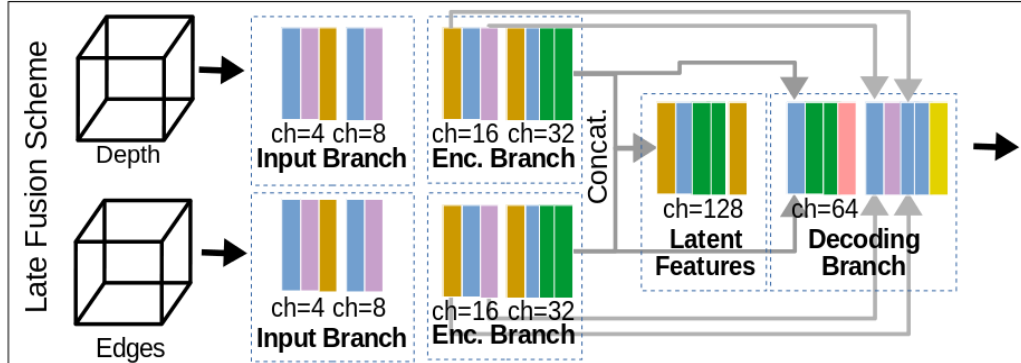
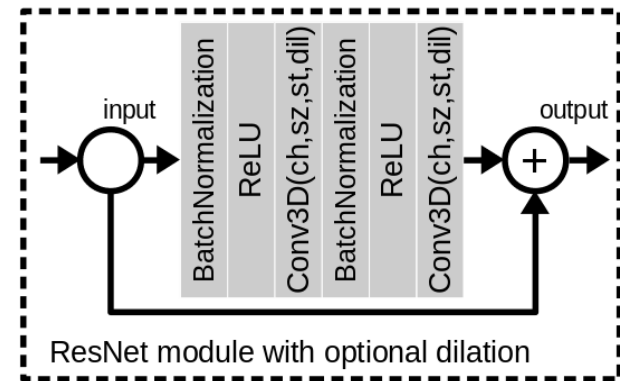
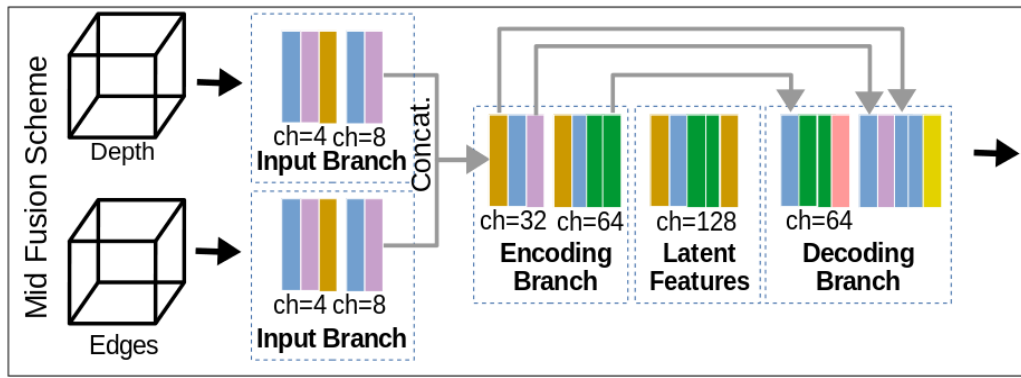
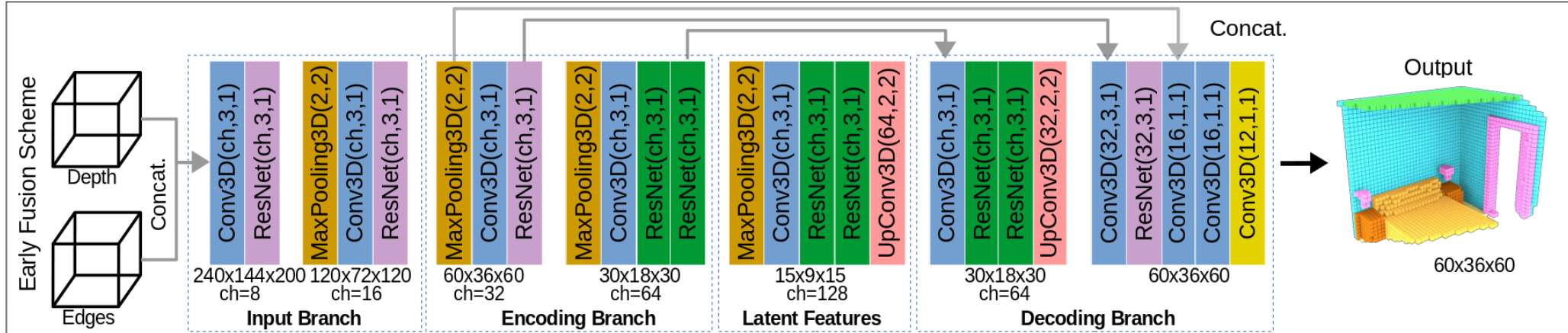
# Network Architecture



# Network Architecture

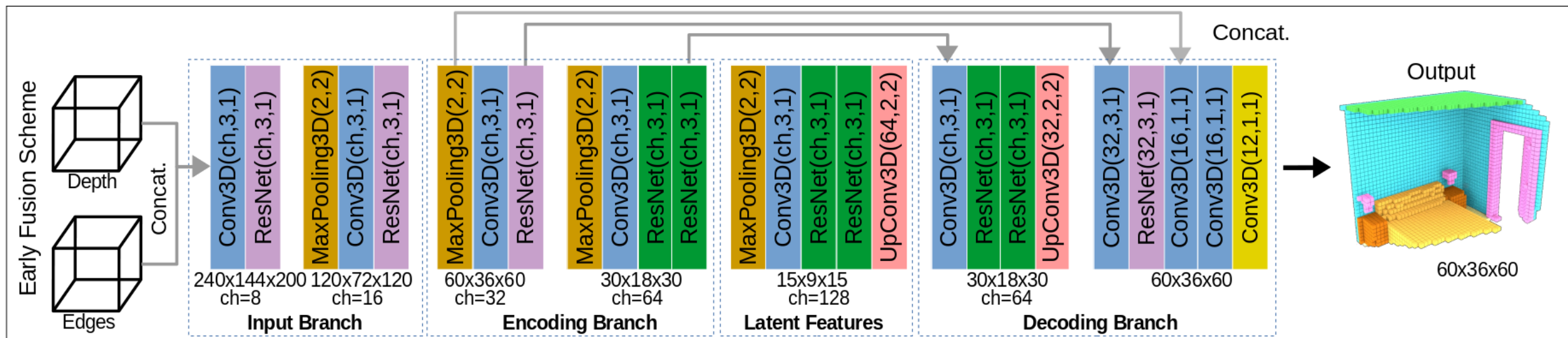


# Network Architecture - Fusion Schemes

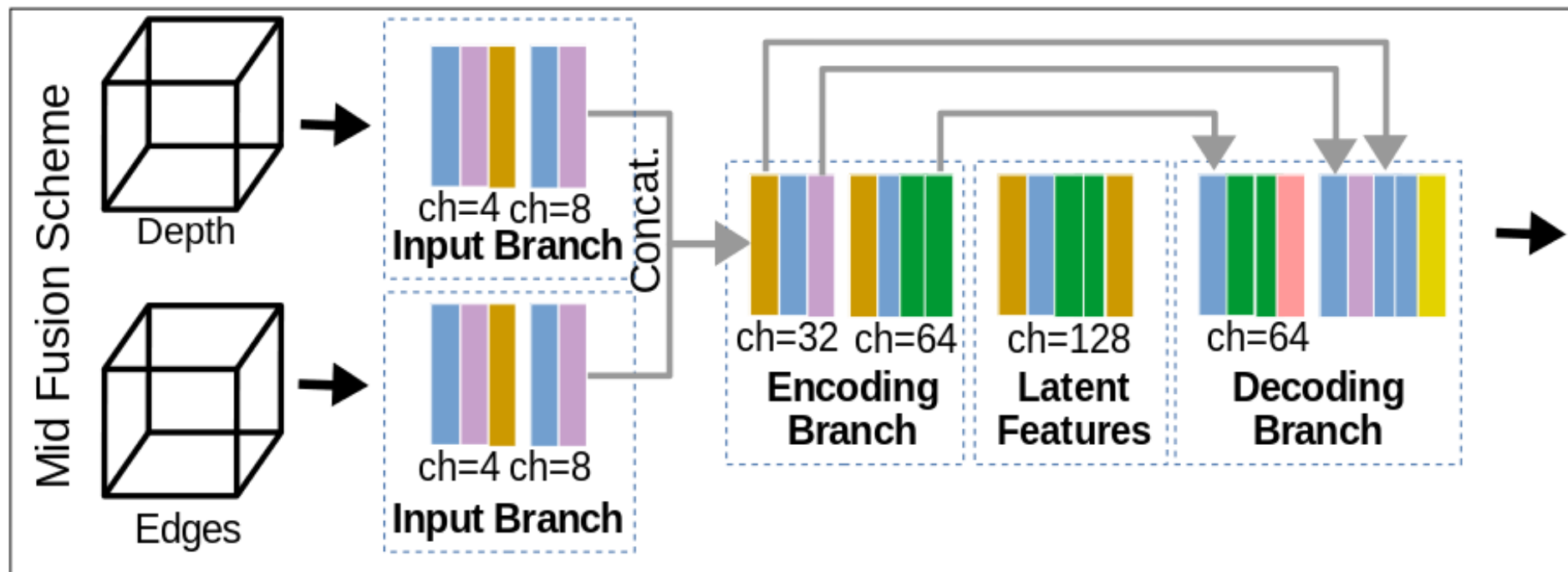


- Conv3D(channels, size, strides)
- ResNet module (channels, size, strides, dilation=1)
- Maxpooling3D(size, strides)
- Dilated ResNet module (channels, size, strides, dilation=2)
- Conv3DTranspose(channels, size, strides)
- Conv3D(channels, size, strides) + Softmax + Categ. Cross Entropy Loss

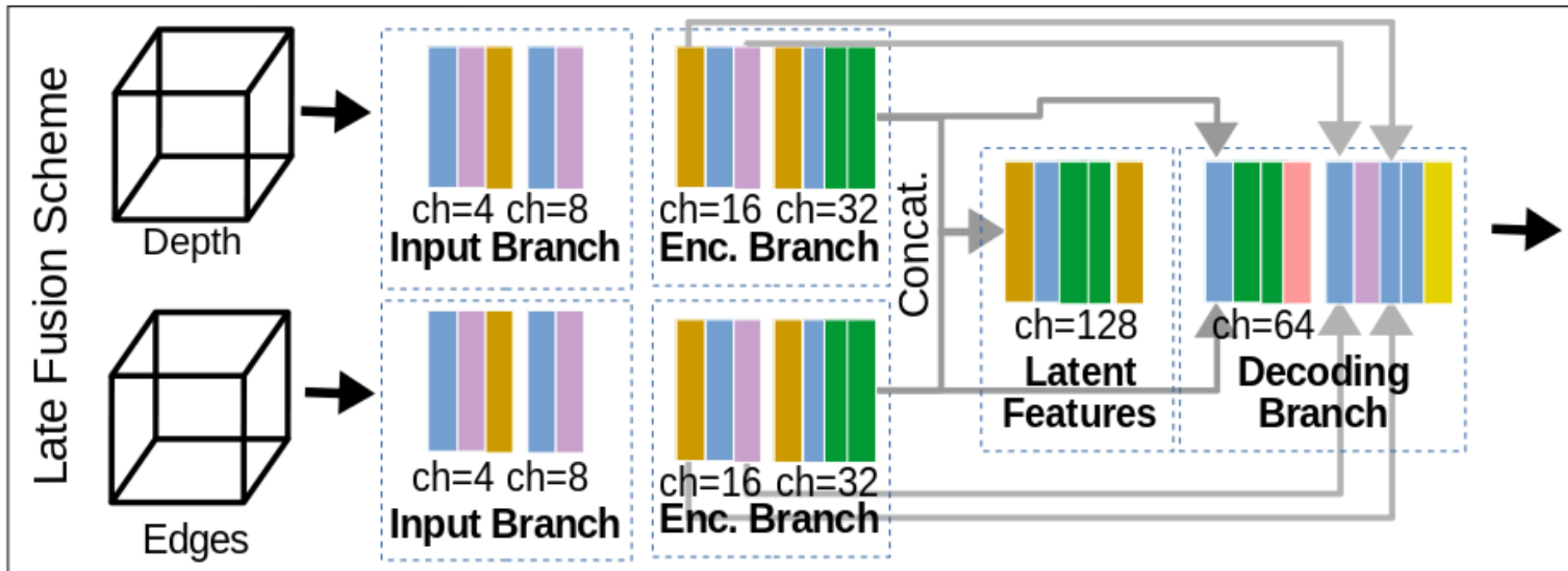
# Network Architecture - Fusion Schemes



# Network Architecture - Fusion Schemes

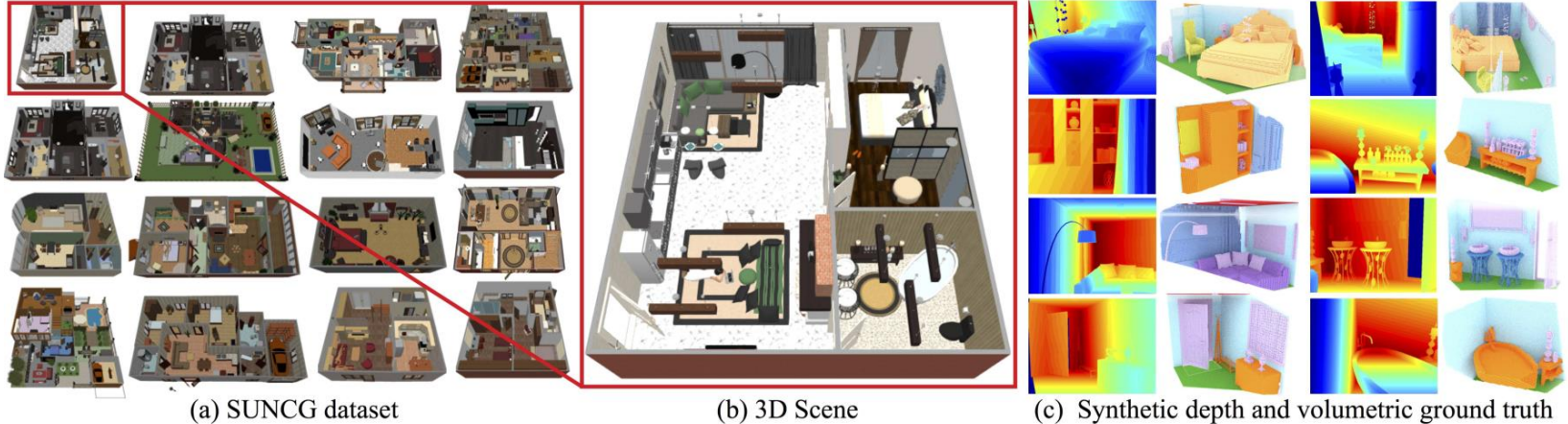


# Network Architecture - Fusion Schemes

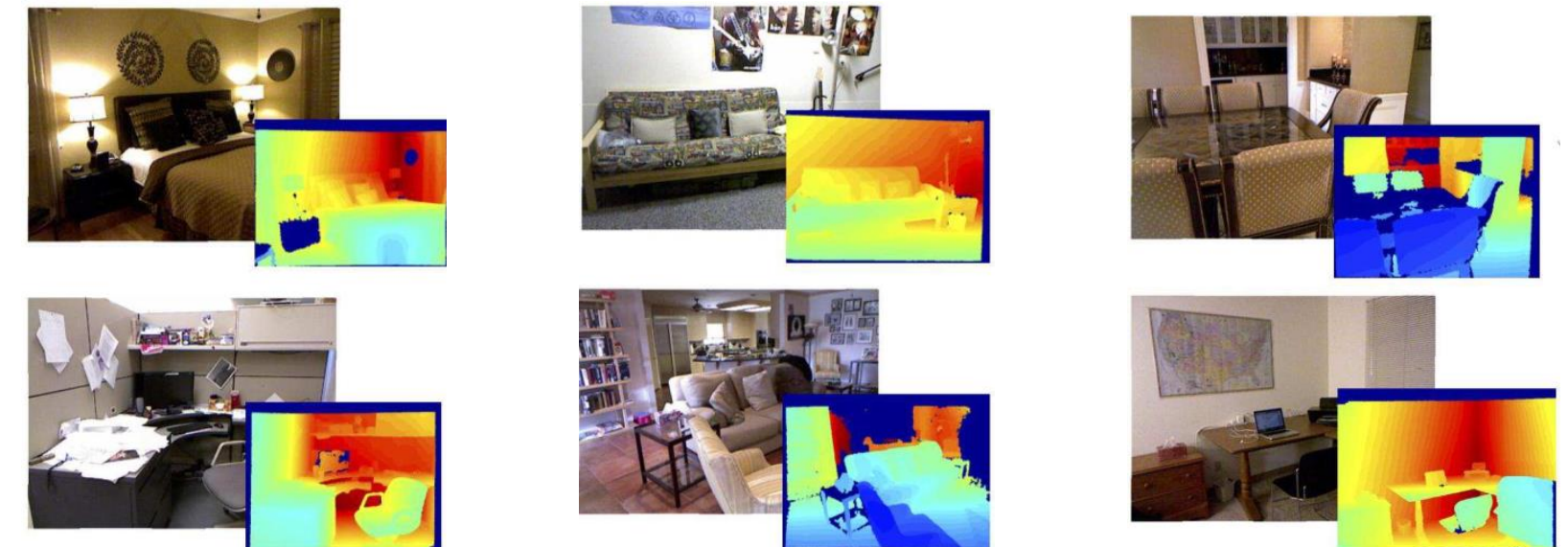


# Datasets

- SUNCG\*



- NYUDv2\*\*



\*Song *et al.*[107]

\*\*Silberman *et al.*[102]

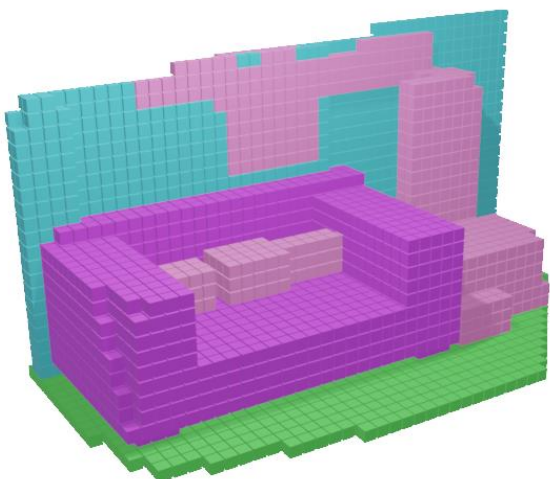
## Training Time

- Ours
  - SUNCG: 4 days
  - NYU: 6 hours
- SSCNET
  - SUNCG: 7 days
  - NYU: 30 hours

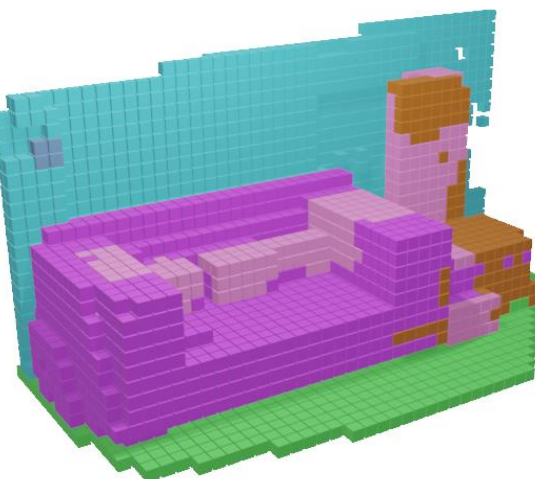
## Quantitative Results

- New state-of-the-art result on SUNCG
- All new aspects of our solution contributed to the improvement
- Middle Fusion and Late Fusion schemes presented similar results on SUNCG
- Middle Fusion presented better results on NYUDV2

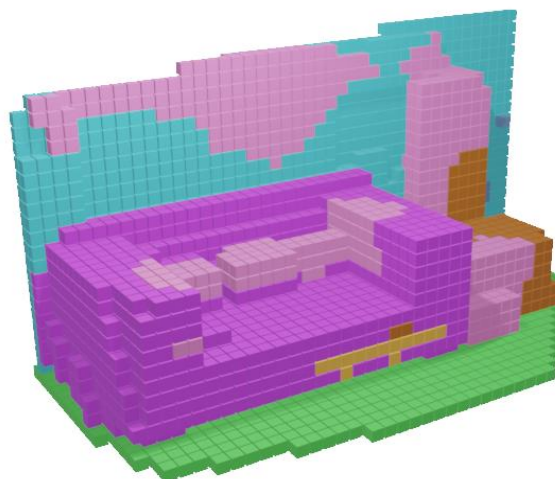
# Qualitative Results



Ground Truth

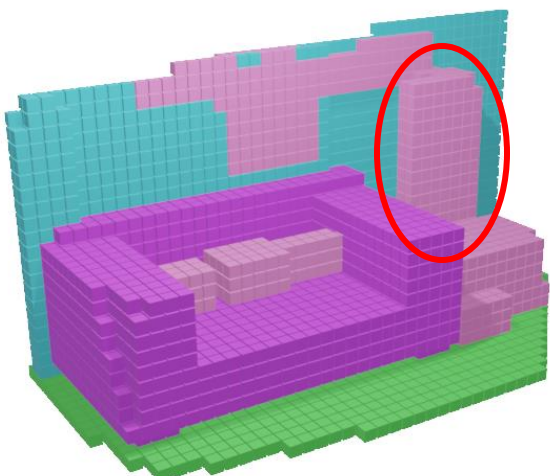


SSCNet

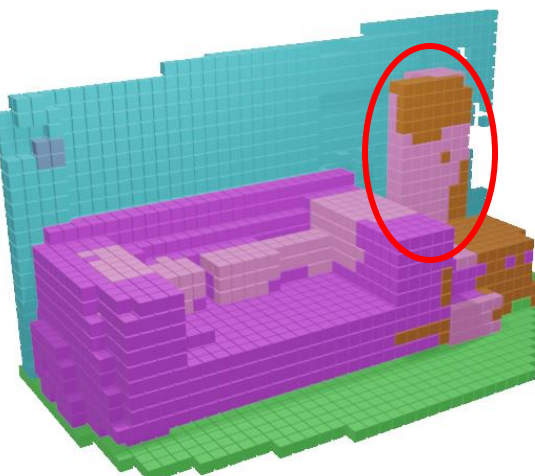


EdgeNet-MF

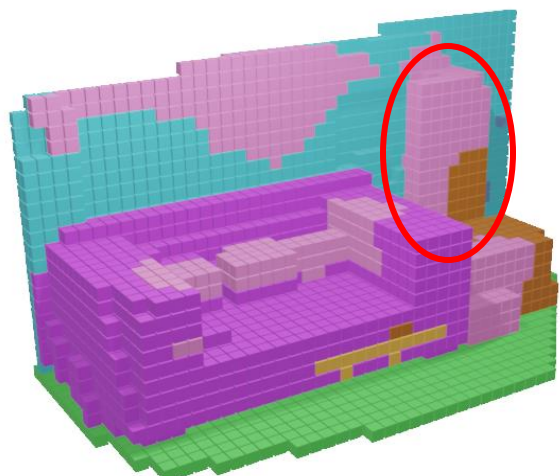
# Qualitative Results



Ground Truth



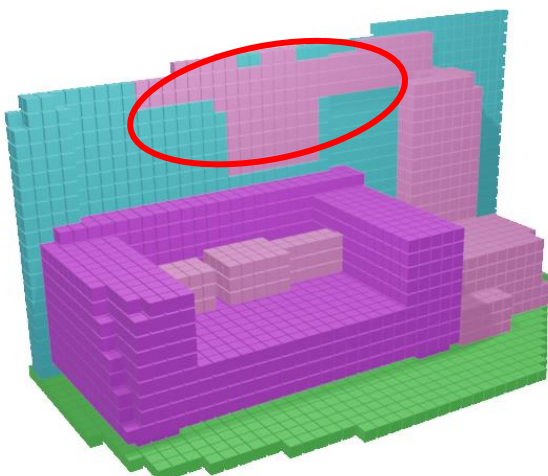
SSCNet



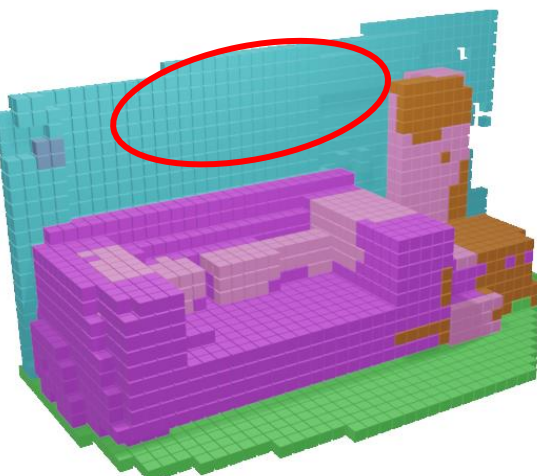
EdgeNet-MF

Higher overall accuracy

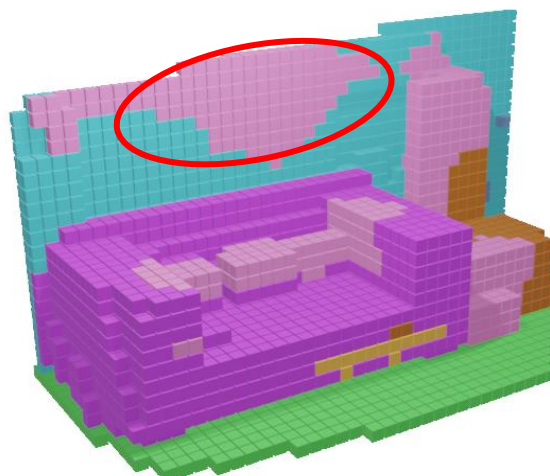
# Qualitative Results



Ground Truth



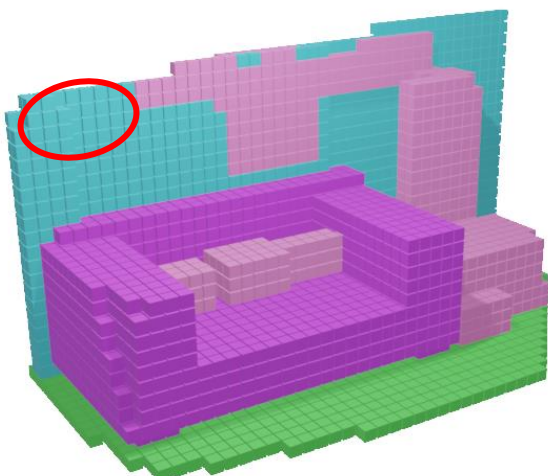
SSCNet



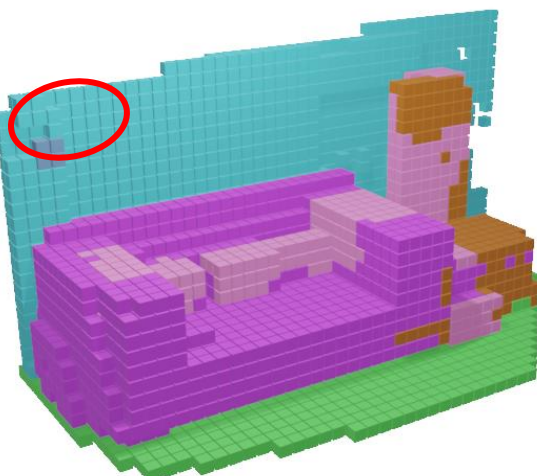
EdgeNet-MF

Hard-to-detect classes

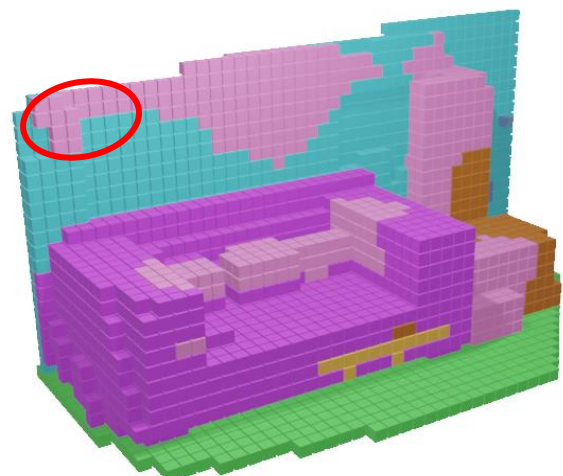
# Qualitative Results



Ground Truth



SSCNet



EdgeNet-MF

NYU Ground Truth errors

## Conclusions

- A new end-to-end network architecture
- A new RGB encoding strategy
- Visually perceptible improvements
- Improvement over the state-of-the-art result on SUNCG
- We surpassed other end-to-end approaches on NYUv2
- An efficient and lightweight training pipeline for the task

# Publication

## *EdgeNet: Semantic Scene Completion from a Single RGB-D Image*

EdgeNet: Semantic Scene Completion from a Single RGB-D Image

Aloisio Dourado, Teófilo Emídio de Campos  
University of Brasília  
Brasília, Brazil  
aloisio.dourado.bb@gmail.com, tdecamps@st-annes.oxon.org

Hansung Kim, Adrian Hilton  
University of Surrey  
Surrey, UK  
(h.kim, a.hilton)@surrey.ac.uk

**Abstract**—Semantic scene completion is the task of predicting a complete 3D representation of a scene from a single point of view. In this paper, we present EdgeNet, a new end-to-end neural network architecture that fuses information from depth and RGB, explicitly representing RGB edge in 3D space. Previous works in this field have used either depth-only or with colour only, proposing 2D semantic labels generated by a 2D segmentation network into the 3D volume, requiring a two step training process. Our EdgeNet representation encodes colour information in 3D space using edge detection and flipped truncated signed distance, which improves semantic completion scores especially for detect classes. We achieved state-of-the-art scores on both synthetic and real datasets with a simpler and a more computationally efficient training pipeline than competing approaches.

**I. INTRODUCTION**

The ability of reasoning about scenes in 3D is a natural task for humans, but remains a challenging problem in Computer Vision [1]. Knowing the complete 3D geometry of a scene and the semantic labels of each 3D voxel has many practical applications, like robotics and autonomous navigation in indoor environments, surveillance, assistive computing and augmented reality.

Currently available low cost RGB-D sensors generate data form a single viewing position and cannot handle occlusion among objects in the scene. For instance, in the scene depicted on the left part of Figure 1, parts of the wall, floor and furniture are occluded by the bed. There is also self-occlusion: the interior of the bed, its sides and its rear surfaces are hidden by the visible surface.

Given a partial 3D scene model acquired from a single RGB-D image, the goal of scene completion is to generate a complete 3D volumetric representation where each voxel is labelled as occupied by some object or free space. For occupied voxels, the goal of semantic scene completion is to assign a label that indicates to which class of object it belongs, as illustrated on the right part of Figure 1.

Before 2018, most of the work on scene reasoning only partially addresses this problem. A number of approaches only infer labels of the visible surfaces [2], [3], [4], while others only consider completing the occluded part of the scene, without semantic labelling [5]. Another line of work focuses on single objects, without the scene context [6].

The term semantic scene completion was introduced by Song *et al.* [7], who showed that scene completion and semantic labelling are intertwined and training a CNN to jointly deal with both tasks can lead to better results. Their approach only uses depth information, ignoring all information from RGB channels. Colour information is expected to be useful to distinguish objects that approximately share the same plane in the 3D space, and thus, are hard to be distinguished using only depth. Examples of such instances are flat objects attached to the wall, such as posters, paintings and flat TVs. Some types of closed doors and windows are also problematic for depth-only approaches.

Recent research also explored colour information from RGB-D images to improve semantic scene completion scores. Some methods project colour information to 3D in a naive way, leading to a problem of data sparsity in the voxelised data that is fed to the 3D CNN [8], while others uses RGB information to train a 2D segmentation network and then project generated features to 3D, requiring a complex two step training process [9], [10].

Our work focuses on enhancing semantic scene segmentation scores using information from both depth and colour of RGB-D images in an end-to-end manner. In order to address the RGB data sparsity issue, we introduce a new strategy for encoding information extracted from RGB image in 3D space. We also present a new end-to-end 3D CNN architecture to combine and represent the features from colour and depth. Comprehensive experiments are conducted to evaluate the main aspects of the proposed solution. Results show that our fusion approach can enhance results of depth-only solutions and that EdgeNet achieves equivalent performance to current state-of-the-art fusion approach, with a much simpler training protocol.

To summarise, our main contributions are:

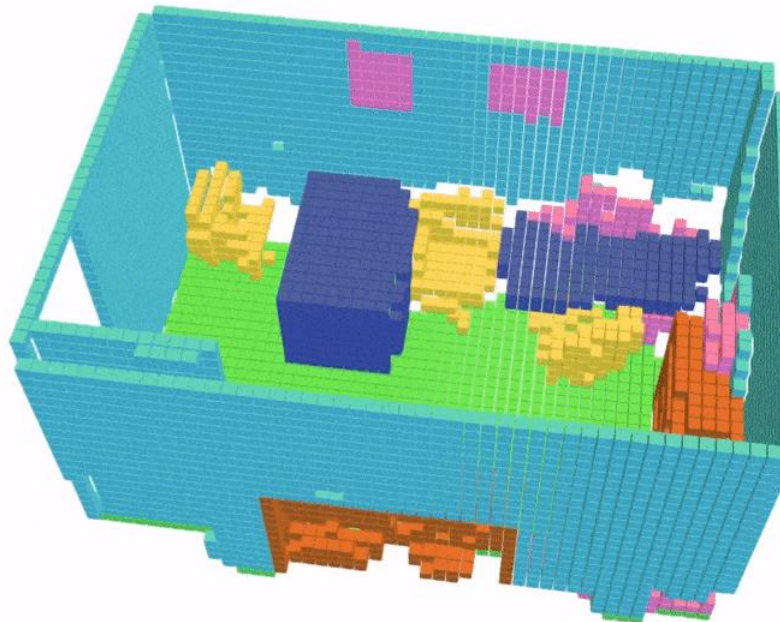
- EdgeNet, a new end-to-end CNN architecture that fuses depth, RGB edge information to achieve state-of-the-art performance in semantic scene completion with a much simpler approach;
- a new 3D volumetric edge representation using flipped signed-distance functions which improves performance and enables data aggregation for semantic scene completion from RGBD;

\*Accepted for publication in the proceedings of the 25<sup>th</sup> International Conference on Pattern Recognition (ICPR2020) (Capes Qualis A2)

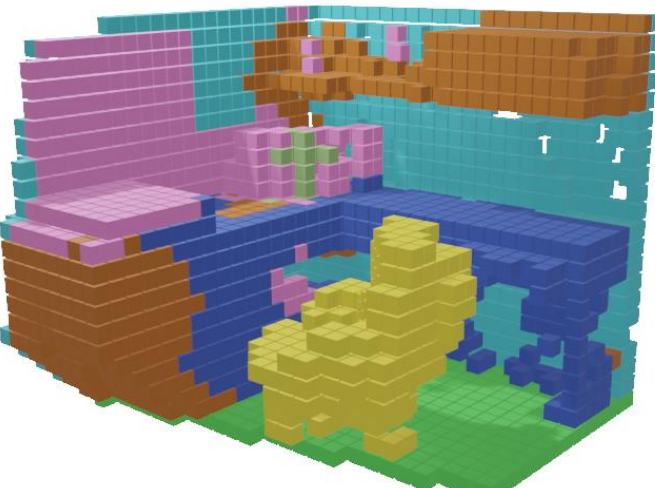
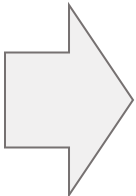
[29] Dourado, A., de Campos, T.E., Kim, H., and Hilton, A.: EdgeNet: Semantic scene completion from RGB-D images. Tech. Rep. arXiv:1908.02893, Cornell University Library, 2019. <http://arxiv.org/abs/1908.02893>. 6, 44, 68

# Chapter 5

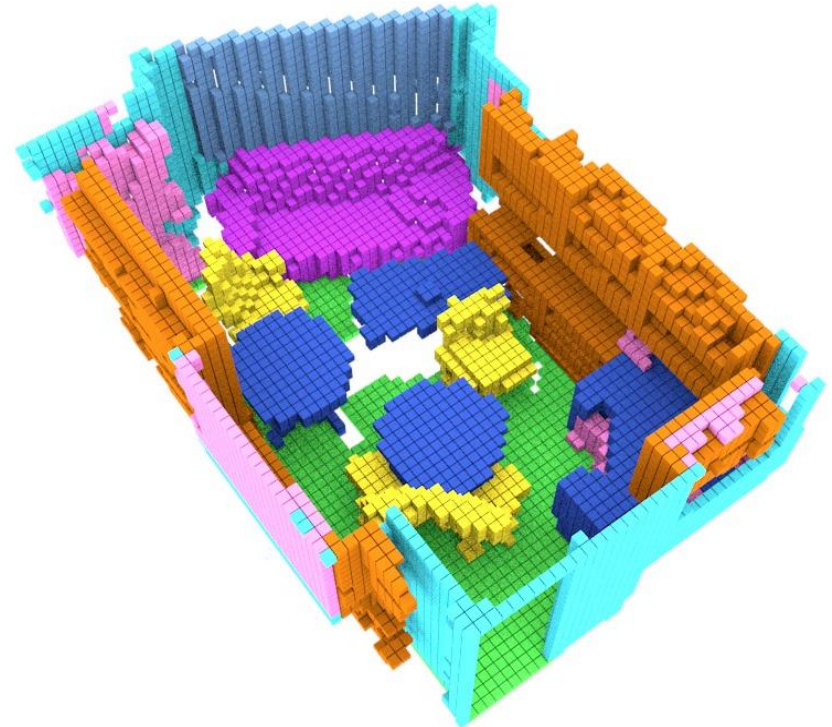
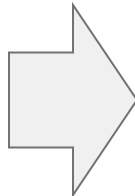
## Extending Semantic Scene Completion for 360° Coverage



# Current Semantic Scene Completion Limitations

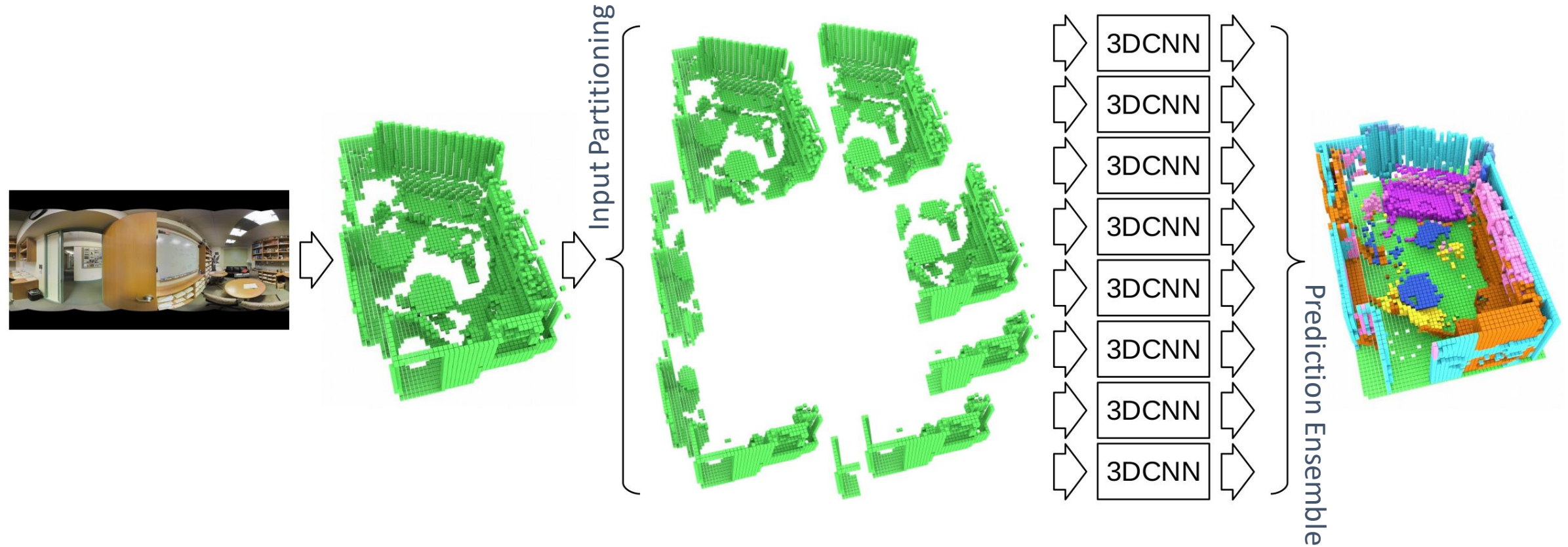


Regular RGB-D Sensor



Panoramic Image from  
Matterport Camera

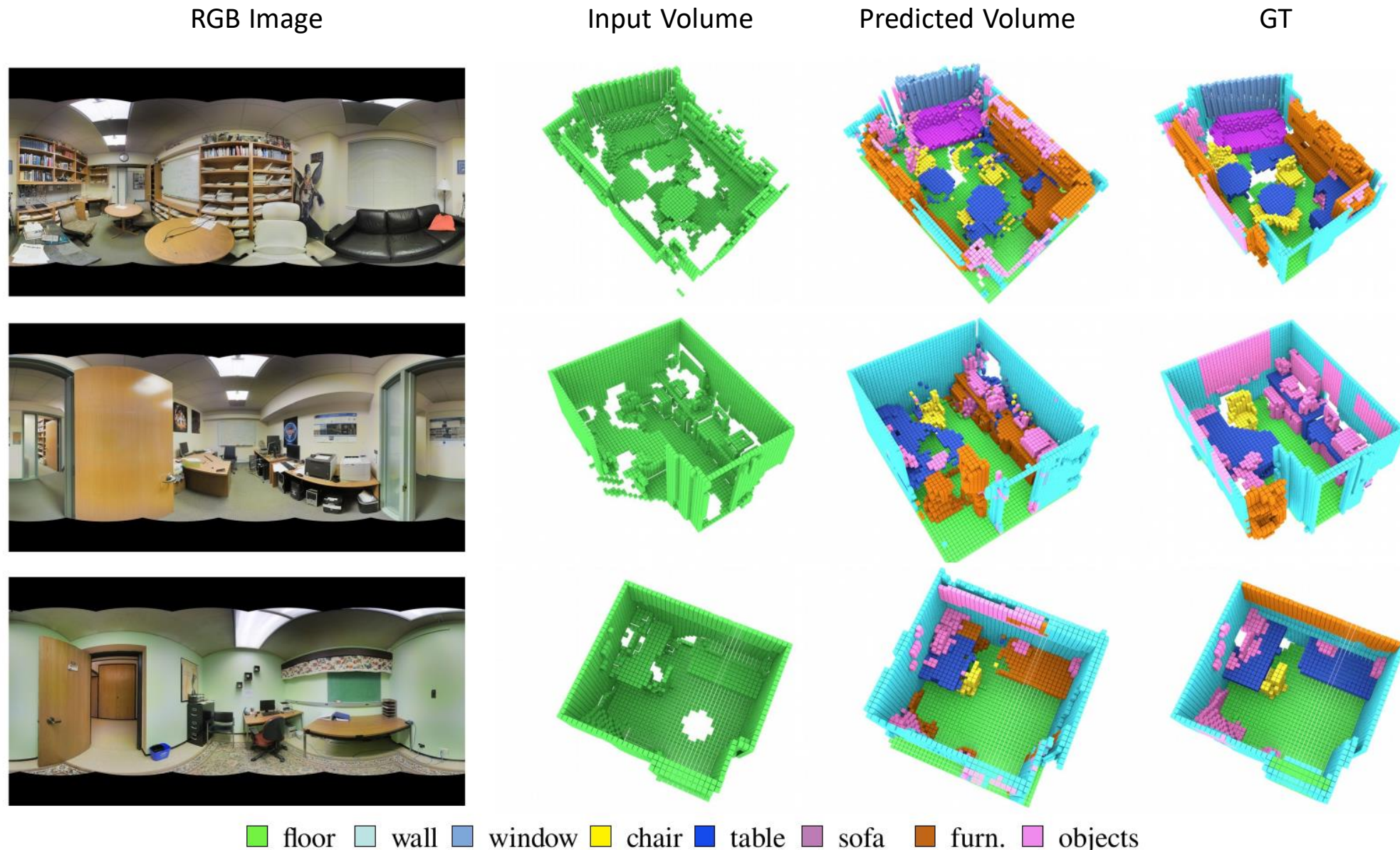
# Our approach



The 3DCNN is trained using SUNCG and fine-tuned in NYUDV2

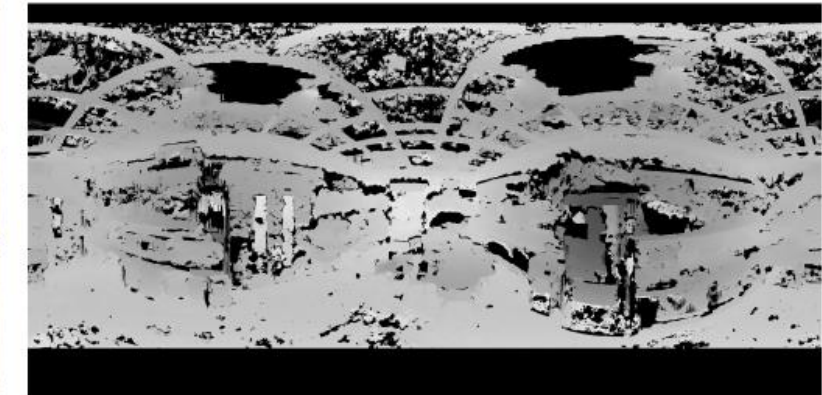
This approach allows to use existing large and diverse RGB-D datasets for training.

# Results on Stanford 2D-3DS Dataset



# Experiments on Spherical Stereo Images

- Stereo capture using commercial 360° cameras is one realistic approach to 360° SSC
- faster compared to Matterport scanning
- depth estimation is subject to errors due to occlusions between two camera views and correspondence matching errors



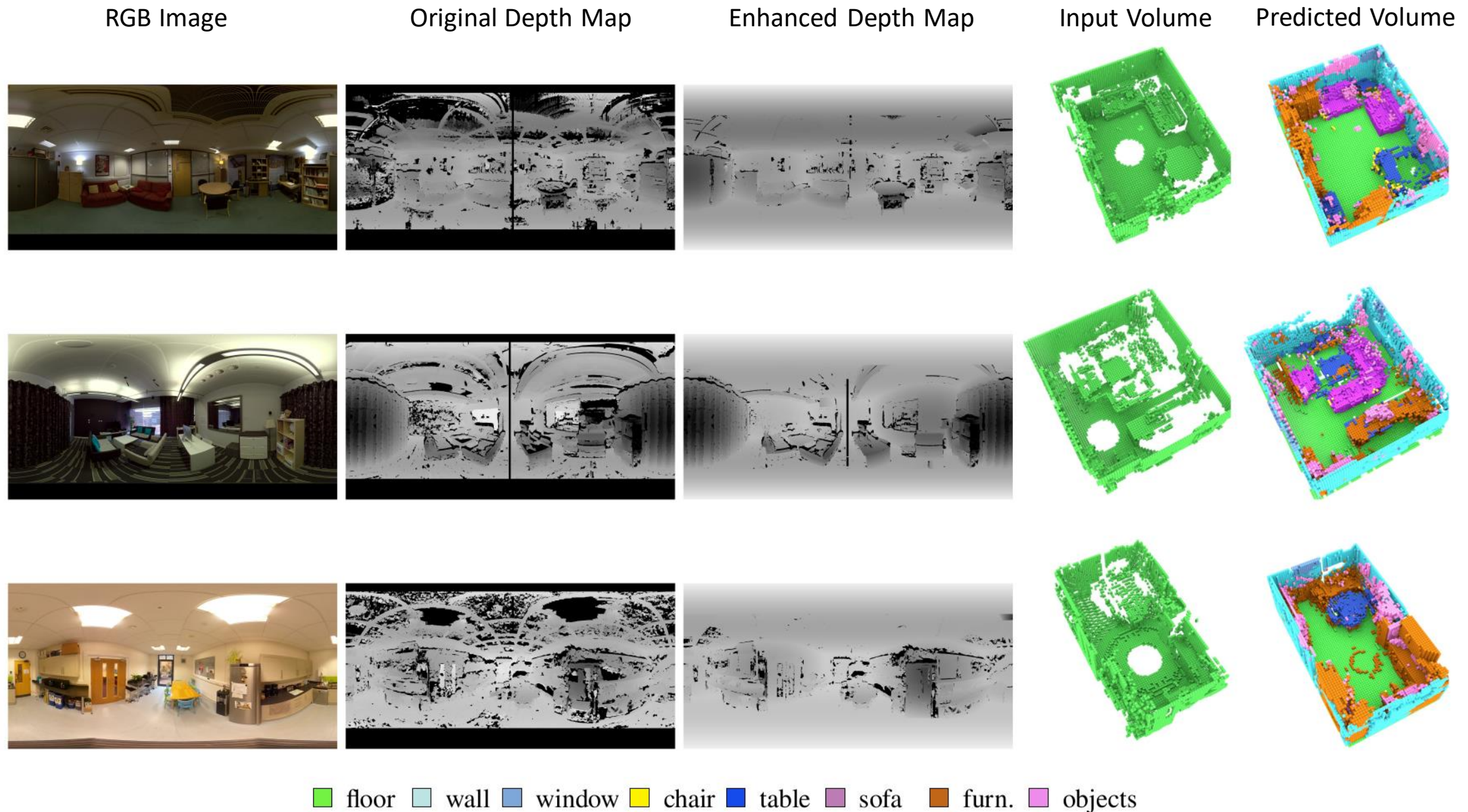
## Our approach

- vertical stereo setup
- Dense stereo matching with spherical stereo geometry [56]
- Depth map enhancement procedure:
  - Align the scene (Manhattan principle)
  - Apply Canny Edge Detector
  - RANSAC to fit a plane over coherent regions with similar colors



[56] Kim, H. and Hilton, A.: Block world reconstruction from spherical stereo image pairs. Computer Vision and Image Understanding (CVIU), 139(C):104–121, Oct. 2015, ISSN 1077-3142. <http://dx.doi.org/10.1016/j.cviu.2015.04.001>. 17, 69

# Results on Spherical Images



## Conclusions

- We introduced the 360° Semantic Scene Completion
- Works with high-end sensors or off-the-shelf 360° cameras
- Segmentation accuracy equivalent to limited view solutions
- High levels of completion of occluded regions

# Publication

## Sematic Scene Completion from a Single 360° Image and Depth Map

**Semantic Scene Completion from a Single 360-Degree Image and Depth Map**

Aloisio Dourado<sup>1</sup>\*, Hansung Kim<sup>2</sup>\*, Teofilo E. de Campos<sup>1</sup> and Adrian Hilton<sup>2</sup><sup>4</sup>

<sup>1</sup>University of Brasília, Brasília, Brazil  
<sup>2</sup>CVSSP, University of Surrey, Surrey, U.K.

**Keywords:** Semantic Scene Completion, 360-Degree Scene Reconstruction, Scene Understanding, 360-Degree Stereo Images.

**Abstract:** We present a method for Semantic Scene Completion (SSC) of complete indoor scenes from a single 360° RGB image and corresponding depth map using a Deep Convolution Neural Network that takes advantage of existing datasets of synthetic and real RGB-D images for training. Recent works on SSC only perform occupancy prediction of small regions of the room covered by the field-of-view of the sensor in use, which implies the need of multiple images to cover the whole scene, being an inappropriate method for dynamic scenes. Our approach uses only a single 360° image with its corresponding depth map to infer the occupancy and semantic labels of the whole room. Using one sensor image is important to allow prediction with no previous knowledge of the sensor and enable it to dynamic scenes and environments. We evaluated our method on two 360° image datasets: a high-quality 360° RGB-D dataset gathered with a Matterport sensor and low-quality 360° RGB-D images generated with a pair of commercial 360° cameras and stereo matching. The experiments showed that the proposed pipeline performs SSC not only with Matterport cameras but also with more affordable 360° cameras, which adds a great number of potential applications, including immersive spatial audio reproduction, augmented reality, assistive computing and robotics.

**1 INTRODUCTION**

Automatic understanding of the complete 3D geometry of a indoor scene and the semantics of each occupied 3D voxel is one of essential problems for many applications, such as robotics, surveillance, assistive computing, spatial audio, immersive spatial audio reproduction and others. After years of an active research field, this still remains a formidable challenge in computer vision. Great advances in scene understanding have been observed in the past few years due to the large scale production of inexpensive depth sensors, such as Microsoft Kinect. Public RGB-D datasets have been created and widely used for many 3D tasks, including prediction of unobserved voxels (Firman et al., 2016), segmentation of visible surface (Silberman and Fergus, 2011; Ren et al., 2012; Qi et al., 2017b; Gupta et al., 2013), object detection (Shrivastava and Mula, 2013) and single object completion (Nguyen et al., 2016).

In 2017, a new line of work was introduced, focusing on the complete understanding of the scene: Semantic Scene Completion (SSC) (Song et al., 2017). SSC is the joint prediction of occupation and semantic labels of visible and occluded regions of the scene. The works in this area are mostly based on the use of Convolution Neural Networks (CNNs) trained on both synthetic and real RGB-D data (Garbade et al., 2018; Guedes et al., 2017; Zhang et al., 2018a; Zhang et al., 2018b; Liu et al., 2018). However, due to the limited field-of-view (FOV) of RGB-D sensors, those methods only predict semantic labels for a small part of the room, and at least four images are required to understand the whole scene.

This scenario recently started to change with the use of more advanced technology for large-scale 3D scanning, such as Light Detection and Ranging (LiDAR) sensor and Matterport cameras. LiDAR is one of the most accurate depth ranging devices using a light pulse signal but it acquires only a point cloud set without colour or connectivity. Some recent LiDAR devices provide coloured 3D structure by map-

\* https://orcid.org/0000-0002-8037-7178  
\* https://orcid.org/0000-0003-4907-0491  
\* https://orcid.org/0000-0001-6172-0229  
\* https://orcid.org/0003-4223-238X

Dourado A, Kim H, E. de Campos, T. and Hilton, A.  
Semantic Scene Completion from a Single 360-Degree Image and Depth Map.  
DOI: 10.2323/000800877703030546  
In Proceedings of the 15th International Joint Conference on Computer Vision, Imaging and Computer Graphics Theory and Applications (VISIGRAPP 2020); pages 36-46.  
ISBN: 978-989-758-402-2  
Copyright © 2020 by SCITEPRESS - Science and Technology Publications, Lda. All rights reserved.

\*Published in the proceedings of the 15<sup>th</sup> International Conference on Computer Vision Theory and Applications (VISAPP2020) (Qualis A1)

[31] Dourado, A., Kim, H., de Campos, T.E., and Hilton, A.: Semantic scene completion from a single 360-degree image and depth map. In Proceedings of the 15th International Joint Conference on Computer Vision, Imaging and Computer Graphics Theory and Applications (VISIGRAPP 2020), vol. 5: VISAPP, pp. 36–46. 7, 61

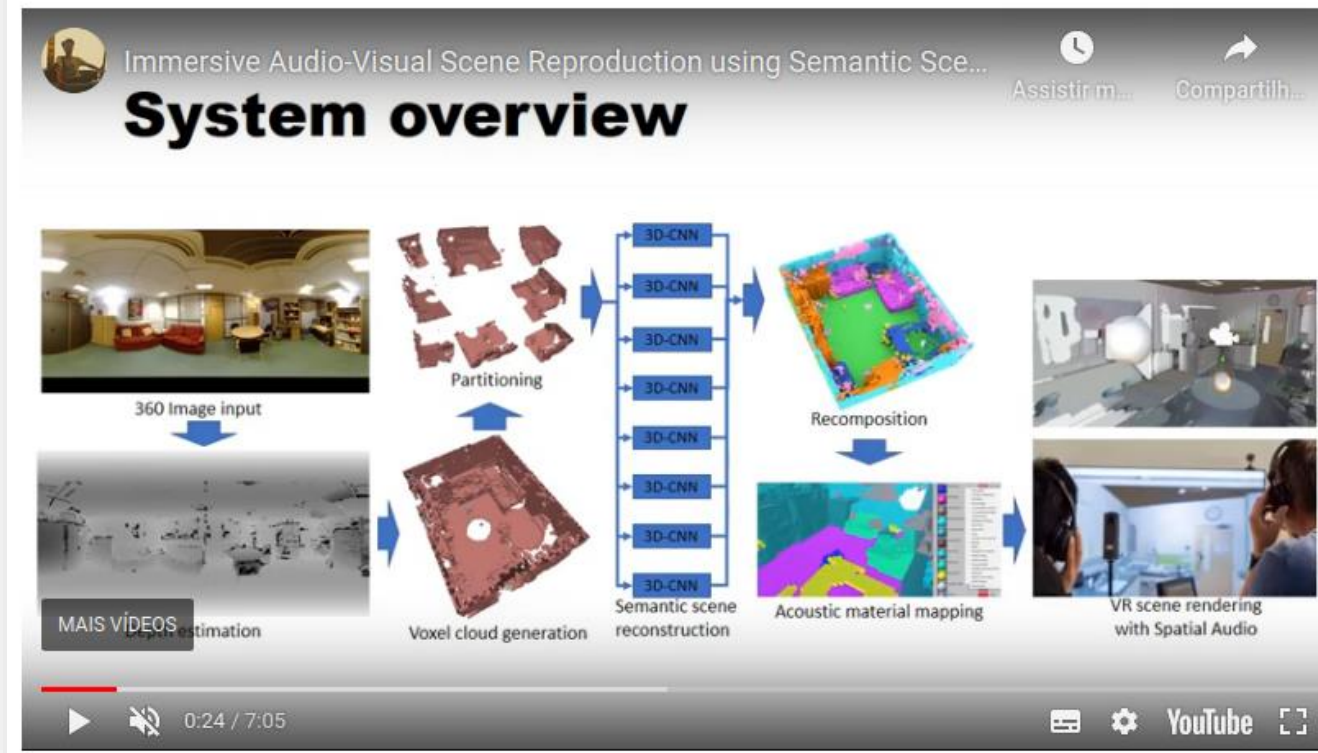
# Application Paper

## *Immersive Audio-Visual Scene Reproduction using Semantic Scene Reconstruction from 360° Cameras*

### **Immersive Audio-Visual Scene Reproduction using Semantic Scene Reconstruction from 360 Cameras**

Hansung Kim, Luca Remaggi, Aloisio Dourado Neto, Teo de Campos, Philip J.B. Jackson and Adrian Hilton

Centre for Vision, Speech & Signal Processing  
University of Surrey, United Kingdom



<https://www.cvssp.org/hkim/paper/CVST2020/>

# Chapter 6

## Work Plan

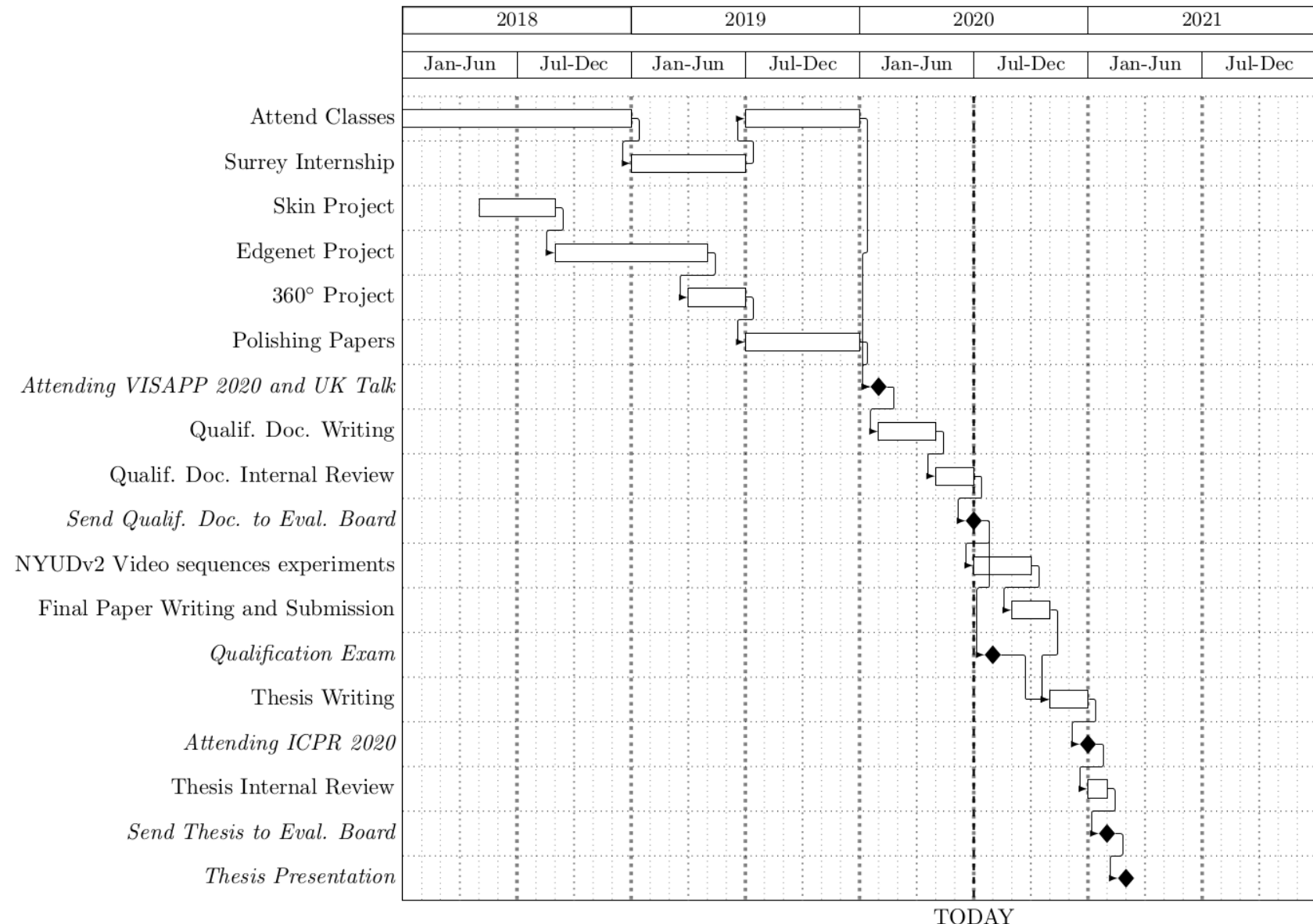
---



## Remaining Activities

- Review the most recent works on the subject
  - evaluate possible ways to improve EdgeNet (Chapter 4)
- Missing experiments:
  - try an offline very late fusion approach
  - train the 360<sup>0</sup> solution on Stanford and other 360<sup>0</sup> datasets (Chapter 5)
  - Try domain adaptation
    - from synthetic data
    - from NYUDV2
- Consolidate enhanced Chapters 4 and 5 into a Journal submission

# Timeline



Thank you!

# Results – ablation study on SUNCG

input	model	scene completion			semantic scene completion (IoU, in percentages)											
		prec.	rec.	IoU	ceil.	floor	wall	win.	chair	bed	sofa	table	tvs	furn.	objs.	avg.
d	SSCNet[24]	76.3	<b>95.2</b>	73.5	96.3	84.9	56.8	28.2	21.3	56.0	52.7	33.7	10.9	44.3	25.4	46.4
	SSCNet*	92.7	89.7	83.8	97.0	94.6	74.3	51.1	43.7	78.2	70.9	49.5	45.2	61.0	51.3	65.2
	DCRF [25]	–	–	–	95.4	84.3	57.7	24.5	28.2	63.4	55.3	34.5	19.6	45.8	28.7	48.8
	VVNetR-120 [9]	90.8	91.7	84.0	<b>98.4</b>	87.0	61.0	54.8	49.3	83.0	<b>75.5</b>	55.1	43.5	68.8	57.7	66.7
	EdgeNet-D	93.1	90.4	84.8	97.2	94.4	78.4	56.1	50.4	80.5	73.8	54.5	49.8	69.5	59.2	69.5
d+s	SNetFuse[14]	56.7	91.7	53.9	65.5	60.7	50.3	56.4	26.1	47.3	43.7	30.6	37.2	44.9	30.0	44.8
	TNetFuse[14]	53.9	95.2	52.6	60.6	57.3	53.2	52.7	27.4	46.8	53.3	28.6	41.1	44.1	29.0	44.9
d+e	SSCNet-E	92.8	89.6	83.8	97.0	94.5	74.6	51.8	43.9	77.0	70.8	49.3	49.2	62.1	52.0	65.7
	EdgeNet-EF(Ours)	<b>93.7</b>	90.3	<b>85.1</b>	97.2	94.9	<b>78.6</b>	57.4	49.5	80.5	74.4	<b>55.8</b>	51.9	70.1	<b>62.5</b>	<b>70.3</b>
	EdgeNet-MF(Ours)	93.3	90.6	<b>85.1</b>	97.2	<b>95.3</b>	78.2	<b>57.5</b>	<b>51.4</b>	<b>80.7</b>	74.1	54.5	<b>52.6</b>	<b>70.3</b>	60.1	70.2
	EdgeNet-LF(Ours)	93.0	89.6	83.9	97.0	94.6	76.4	52.0	44.6	79.8	71.5	48.9	48.3	66.1	55.9	66.8

# Results – ablation study on SUNCG

input	model	scene completion			semantic scene completion (IoU, in percentages)											
		prec.	rec.	IoU	ceil.	floor	wall	win.	chair	bed	sofa	table	tvs	furn.	objs.	avg.
d	SSCNet[24]	76.3	<b>95.2</b>	73.5	96.3	84.9	56.8	28.2	21.3	56.0	52.7	33.7	10.9	44.3	25.4	46.4
	SSCNet*	92.7	89.7	83.8	97.0	94.6	74.3	51.1	43.7	78.2	70.9	49.5	45.2	61.0	51.3	65.2
	DCRF [25]	–	–	–	95.4	84.3	57.7	24.5	28.2	63.4	55.3	34.5	19.6	45.8	28.7	48.8
	VVNetR-120 [9]	90.8	91.7	84.0	<b>98.4</b>	87.0	61.0	54.8	49.3	83.0	<b>75.5</b>	55.1	43.5	68.8	57.7	66.7
	EdgeNet-D	93.1	90.4	84.8	97.2	94.4	78.4	56.1	50.4	80.5	73.8	54.5	49.8	69.5	59.2	69.5
d+s	SNetFuse[14]	56.7	91.7	53.9	65.5	60.7	50.3	56.4	26.1	47.3	43.7	30.6	37.2	44.9	30.0	44.8
	TNetFuse[14]	53.9	<b>95.2</b>	52.6	60.6	57.3	53.2	52.7	27.4	46.8	53.3	28.6	41.1	44.1	29.0	44.9
d+e	SSCNet-E	92.8	89.6	83.8	97.0	94.5	74.6	51.8	43.9	77.0	70.8	49.3	49.2	62.1	52.0	65.7
	EdgeNet-EF(Ours)	<b>93.7</b>	90.3	<b>85.1</b>	97.2	94.9	<b>78.6</b>	57.4	49.5	80.5	74.4	<b>55.8</b>	51.9	70.1	<b>62.5</b>	<b>70.3</b>
	EdgeNet-MF(Ours)	93.3	90.6	<b>85.1</b>	97.2	<b>95.3</b>	78.2	<b>57.5</b>	<b>51.4</b>	<b>80.7</b>	74.1	54.5	<b>52.6</b>	<b>70.3</b>	60.1	70.2
	EdgeNet-LF(Ours)	93.0	89.6	83.9	97.0	94.6	76.4	52.0	44.6	79.8	71.5	48.9	48.3	66.1	55.9	66.8

Effect of our efficient training pipeline

# Results – ablation study on SUNCG

input	model	scene completion			semantic scene completion (IoU, in percentages)											
		prec.	rec.	IoU	ceil.	floor	wall	win.	chair	bed	sofa	table	tvs	furn.	objs.	avg.
d	SSCNet[24]	76.3	<b>95.2</b>	73.5	96.3	84.9	56.8	28.2	21.3	56.0	52.7	33.7	10.9	44.3	25.4	46.4
	SSCNet*	92.7	89.7	83.8	97.0	94.6	74.3	51.1	43.7	78.2	70.9	49.5	45.2	61.0	51.3	65.2
	DCRF [25]	–	–	–	95.4	84.3	57.7	24.5	28.2	63.4	55.3	34.5	19.6	45.8	28.7	48.8
	VVNetR-120 [9]	90.8	91.7	84.0	<b>98.4</b>	87.0	61.0	54.8	49.3	83.0	<b>75.5</b>	55.1	43.5	68.8	57.7	66.7
	EdgeNet-D	93.1	90.4	84.8	97.2	94.4	78.4	56.1	50.4	80.5	73.8	54.5	49.8	69.5	59.2	69.5
d+s	SNetFuse[14]	56.7	91.7	53.9	65.5	60.7	50.3	56.4	26.1	47.3	43.7	30.6	37.2	44.9	30.0	44.8
	TNetFuse[14]	53.9	95.2	52.6	60.6	57.3	53.2	52.7	27.4	46.8	53.3	28.6	41.1	44.1	29.0	44.9
d+e	SSCNet-E	92.8	89.6	83.8	97.0	94.5	74.6	51.8	43.9	77.0	70.8	49.3	49.2	62.1	52.0	65.7
	EdgeNet-EF(Ours)	<b>93.7</b>	90.3	<b>85.1</b>	97.2	94.9	<b>78.6</b>	57.4	49.5	80.5	74.4	<b>55.8</b>	51.9	70.1	<b>62.5</b>	<b>70.3</b>
	EdgeNet-MF(Ours)	93.3	90.6	<b>85.1</b>	97.2	<b>95.3</b>	78.2	<b>57.5</b>	<b>51.4</b>	<b>80.7</b>	74.1	54.5	<b>52.6</b>	<b>70.3</b>	60.1	70.2
	EdgeNet-LF(Ours)	93.0	89.6	83.9	97.0	94.6	76.4	52.0	44.6	79.8	71.5	48.9	48.3	66.1	55.9	66.8

Effect of our u-shaped architecture, with 3D dilated residual modules

# Results – ablation study on SUNCG

input	model	scene completion			semantic scene completion (IoU, in percentages)											
		prec.	rec.	IoU	ceil.	floor	wall	win.	chair	bed	sofa	table	tvs	furn.	objs.	avg.
d	SSCNet[24]	76.3	<b>95.2</b>	73.5	96.3	84.9	56.8	28.2	21.3	56.0	52.7	33.7	10.9	44.3	25.4	46.4
	SSCNet*	92.7	89.7	83.8	97.0	94.6	74.3	51.1	43.7	78.2	70.9	49.5	45.2	61.0	51.3	65.2
	DCRF [25]	–	–	–	95.4	84.3	57.7	24.5	28.2	63.4	55.3	34.5	19.6	45.8	28.7	48.8
	VVNetR-120 [9]	90.8	91.7	84.0	<b>98.4</b>	87.0	61.0	54.8	49.3	83.0	<b>75.5</b>	55.1	43.5	68.8	57.7	66.7
	EdgeNet-D	93.1	90.4	84.8	97.2	94.4	78.4	56.1	50.4	80.5	73.8	54.5	49.8	69.5	59.2	<b>69.5</b>
d+s	SNetFuse[14]	56.7	91.7	53.9	65.5	60.7	50.3	56.4	26.1	47.3	43.7	30.6	37.2	44.9	30.0	44.8
	TNetFuse[14]	53.9	95.2	52.6	60.6	57.3	53.2	52.7	27.4	46.8	53.3	28.6	41.1	44.1	29.0	44.9
d+e	SSCNet-E	92.8	89.6	83.8	97.0	94.5	74.6	51.8	43.9	77.0	70.8	49.3	49.2	62.1	52.0	<b>65.7</b>
	EdgeNet-EF(Ours)	<b>93.7</b>	90.3	<b>85.1</b>	97.2	94.9	<b>78.6</b>	57.4	49.5	80.5	74.4	<b>55.8</b>	51.9	70.1	<b>62.5</b>	<b>70.3</b>
	EdgeNet-MF(Ours)	93.3	90.6	<b>85.1</b>	97.2	<b>95.3</b>	78.2	<b>57.5</b>	<b>51.4</b>	<b>80.7</b>	74.1	54.5	<b>52.6</b>	<b>70.3</b>	60.1	70.2
	EdgeNet-LF(Ours)	93.0	89.6	83.9	97.0	94.6	76.4	52.0	44.6	79.8	71.5	48.9	48.3	66.1	55.9	66.8

Effect of adding edges

# Results – ablation study on SUNCG

input	model	scene completion			semantic scene completion (IoU, in percentages)											
		prec.	rec.	IoU	ceil.	floor	wall	win.	chair	bed	sofa	table	tvs	furn.	objs.	avg.
d	SSCNet[24]	76.3	<b>95.2</b>	73.5	96.3	84.9	56.8	28.2	21.3	56.0	52.7	33.7	10.9	44.3	25.4	46.4
	SSCNet*	92.7	89.7	83.8	97.0	94.6	74.3	51.1	43.7	78.2	70.9	49.5	45.2	61.0	51.3	65.2
	DCRF [25]	–	–	–	95.4	84.3	57.7	24.5	28.2	63.4	55.3	34.5	19.6	45.8	28.7	48.8
	VVNetR-120 [9]	90.8	91.7	84.0	<b>98.4</b>	87.0	61.0	54.8	49.3	83.0	<b>75.5</b>	55.1	43.5	68.8	57.7	66.7
	EdgeNet-D	93.1	90.4	84.8	97.2	94.4	78.4	<b>56.1</b>	50.4	80.5	73.8	54.5	<b>49.8</b>	69.5	<b>59.2</b>	<b>69.5</b>
d+s	SNetFuse[14]	56.7	91.7	53.9	65.5	60.7	50.3	56.4	26.1	47.3	43.7	30.6	37.2	44.9	30.0	44.8
	TNetFuse[14]	53.9	95.2	52.6	60.6	57.3	53.2	52.7	27.4	46.8	53.3	28.6	41.1	44.1	29.0	44.9
d+e	SSCNet-E	92.8	89.6	83.8	97.0	94.5	74.6	<b>51.8</b>	43.9	77.0	70.8	49.3	<b>49.2</b>	62.1	<b>52.0</b>	<b>65.7</b>
	EdgeNet-EF(Ours)	<b>93.7</b>	90.3	<b>85.1</b>	97.2	94.9	<b>78.6</b>	<b>57.4</b>	49.5	80.5	74.4	<b>55.8</b>	<b>51.9</b>	70.1	<b>62.5</b>	<b>70.3</b>
	EdgeNet-MF(Ours)	93.3	90.6	<b>85.1</b>	97.2	<b>95.3</b>	78.2	<b>57.5</b>	<b>51.4</b>	<b>80.7</b>	74.1	54.5	<b>52.6</b>	<b>70.3</b>	60.1	70.2
	EdgeNet-LF(Ours)	93.0	89.6	83.9	97.0	94.6	76.4	52.0	44.6	79.8	71.5	48.9	48.3	66.1	55.9	66.8

Effect of adding edges

# Results on NYU-DV2

input	model	scene completion			semantic scene completion (IoU, in percentages)											
		prec.	rec.	IoU	ceil.	floor	wall	win.	chair	bed	sofa	table	tvs	furn.	objs.	avg.
d	SSCNet[24]	76.3	<b>95.2</b>	73.5	96.3	84.9	56.8	28.2	21.3	56.0	52.7	33.7	10.9	44.3	25.4	46.4
	SSCNet*	92.7	89.7	83.8	97.0	94.6	74.3	51.1	43.7	78.2	70.9	49.5	45.2	61.0	51.3	65.2
	DCRF [25]	–	–	–	95.4	84.3	57.7	24.5	28.2	63.4	55.3	34.5	19.6	45.8	28.7	48.8
	VVNetR-120 [9]	90.8	91.7	84.0	<b>98.4</b>	87.0	61.0	54.8	49.3	83.0	<b>75.5</b>	55.1	43.5	68.8	57.7	66.7
	EdgeNet-D	93.1	90.4	84.8	97.2	94.4	78.4	56.1	50.4	80.5	73.8	54.5	49.8	69.5	59.2	69.5
d+s	SNetFuse[14]	56.7	91.7	53.9	65.5	60.7	50.3	56.4	26.1	47.3	43.7	30.6	37.2	44.9	30.0	44.8
	TNetFuse[14]	53.9	95.2	52.6	60.6	57.3	53.2	52.7	27.4	46.8	53.3	28.6	41.1	44.1	29.0	44.9
d+e	SSCNet-E	92.8	89.6	83.8	97.0	94.5	74.6	51.8	43.9	77.0	70.8	49.3	49.2	62.1	52.0	65.7
	EdgeNet-EF(Ours)	<b>93.7</b>	90.3	<b>85.1</b>	97.2	94.9	<b>78.6</b>	57.4	49.5	80.5	74.4	<b>55.8</b>	51.9	70.1	<b>62.5</b>	<b>70.3</b>
	EdgeNet-MF(Ours)	93.3	90.6	<b>85.1</b>	97.2	<b>95.3</b>	78.2	<b>57.5</b>	<b>51.4</b>	<b>80.7</b>	74.1	54.5	<b>52.6</b>	<b>70.3</b>	60.1	70.2
	EdgeNet-LF(Ours)	93.0	89.6	83.9	97.0	94.6	76.4	52.0	44.6	79.8	71.5	48.9	48.3	66.1	55.9	66.8

Effect of different fusion strategies

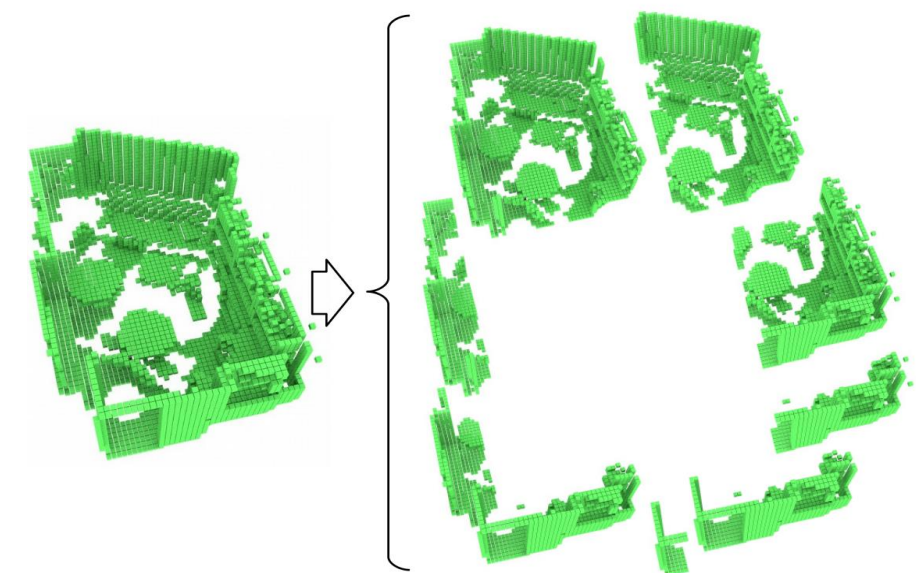
# Results on NYU-DV2

train	input	model	scene completion			semantic scene completion (IoU, in percentages)												
			prec.	rec.	IoU	ceil.	floor	wall	win.	chair	bed	sofa	table	tvs	furn.	objs.	avg.	
SUNCG	d	SSCNet[24]	55.6	91.9	53.2	5.8	81.8	19.6	5.4	12.9	34.4	26	13.6	6.1	9.4	7.4	20.2	
	d+e	EdgeNet-EF(Ours)	<b>61.9</b>	80.0	<b>53.6</b>	9.1	<b>92.9</b>	18.3	5.7	15.8	40.4	30.7	9.2	3.3	13.7	11.6	22.8	
	d+e	EdgeNet-MF(Ours)	60.7	80.3	52.8	<b>11.0</b>	92.3	<b>20.5</b>	7.2	<b>16.3</b>	42.8	<b>32.8</b>	<b>10.5</b>	<b>6.0</b>	<b>15.7</b>	<b>11.8</b>	<b>24.3</b>	
	d+e	EdgeNet-LF(Ours)	59.9	<b>80.5</b>	52.3	3.2	87.1	19.9	<b>8.6</b>	15.4	<b>43.5</b>	32.3	8.8	4.3	13.7	10.0	22.4	
NYU	d	SSCNet[24]	57.0	<b>94.5</b>	55.1	15.1	94.7	24.4	0.0	<b>12.6</b>	32.1	35.0	<b>13.0</b>	<b>7.8</b>	27.1	10.1	24.7	
	d+e	EdgeNet-EF(Ours)	<b>78.1</b>	65.1	55.1	<b>21.8</b>	<b>95.0</b>	27.3	<b>8.4</b>	6.8	<b>53.1</b>	38.6	7.5	0.0	30.4	<b>13.3</b>	27.5	
	d+e	EdgeNet-MF(Ours)	76.0	68.3	<b>56.1</b>	17.9	94.0	<b>27.8</b>	2.1	9.5	51.8	<b>44.3</b>	9.4	3.6	<b>32.5</b>	12.7	<b>27.8</b>	
	d+e	EdgeNet-LF(Ours)	75.5	67.5	55.4	19.8	94.9	24.4	5.7	7.2	50.3	38.8	10.0	0.0	33.2	12.2	27.0	
SUNCG + NYU	d	SSCNet[24]	59.3	92.9	56.6	15.1	94.6	24.7	10.8	17.3	53.2	45.9	15.9	13.9	31.1	12.6	30.5	
	d	DCRF[25]	-	-	-	18.1	92.6	27.1	10.8	18.8	54.3	47.9	17.1	15.1	34.7	13.0	31.8	
	d	VVNetR-120[9]	69.8	83.1	61.1	19.3	94.8	28.0	12.2	19.6	57.0	50.5	17.6	11.9	35.6	15.3	32.9	
	d+c	Guedes <i>et al.</i> [7]	-	-	56.6	-	-	-	-	-	-	-	-	-	-	-	30.5	
	d+s	Garbade <i>et al.</i> *[6]	69.5	82.7	<b>60.7</b>	12.9	92.5	25.3	20.1	16.1	56.3	43.4	17.2	10.4	33.0	14.3	31.0	
	d+s	SNetFuse[14]	67.6	<b>85.9</b>	<b>60.7</b>	22.2	91.0	28.6	<b>18.2</b>	19.2	56.2	51.2	16.2	12.2	37.0	17.4	33.6	
	d+e	TNetFuse[14]	67.3	85.8	<b>60.7</b>	17.3	92.1	28.0	16.6	19.3	<b>57.5</b>	<b>53.8</b>	<b>17.7</b>	<b>18.5</b>	<b>38.4</b>	<b>18.9</b>	<b>34.4</b>	
	d+e	EdgeNet-EF(Ours)	77.0	70.0	57.9	16.3	<b>95.0</b>	27.9	14.2	17.9	55.4	50.8	16.5	6.8	37.3	15.3	32.1	
	d+e	EdgeNet-MF(Ours)	<b>79.1</b>	66.6	56.7	<b>22.4</b>	<b>95.0</b>	<b>29.7</b>	15.5	<b>20.9</b>	54.1	53.0	15.6	14.9	35.0	14.8	33.7	
	d+e	EdgeNet-LF(Ours)	77.6	69.5	57.9	20.6	94.9	29.5	9.8	18.1	56.2	50.5	11.4	5.2	35.9	15.3	31.6	

# Our approach

- Input volume:
  - $480 \times 144 \times 480$  voxels
  - Voxel size: 0.02m
  - coverage:  $9.6 \times 2.8 \times 9.6$  m
- 8 partitions, emulating the field of view of a standard RGB-D sensor
- The partitions are taken from the sensor position, using a  $45^\circ$  step
- We move the point-of-view 1.7m back from the original sensor position, to get more overlapped coverage

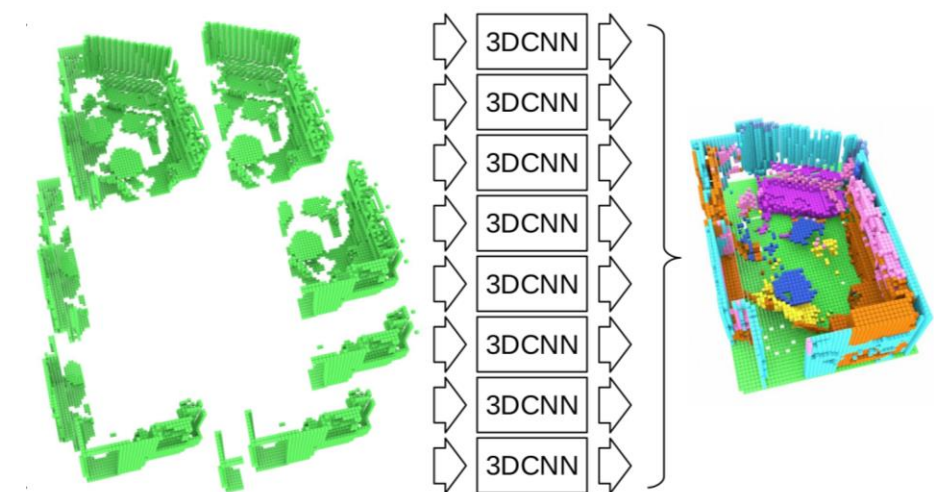
Input Partitioning



# Our approach

- Each partition of the input is processed by our CNN, generating 8 predicted volumes
- Overlapping areas are ensembled using the sum rule
- Each predicted partition size is  $60 \times 36 \times 60$
- The resulting ensembled volume size is  $120 \times 36 \times 120$

Prediction Ensemble



# Results on Stanford 2D-3DS Dataset

evaluation dataset	model	scene coverage	semantic scene completion (IoU, in percentages)											
			ceil.	floor	wall	win.	chair	bed	sofa	table	tvs	furn.	objs.	avg.
NYU v2 RGB-D	SSCNet	partial	15.1	94.6	24.7	10.8	17.3	53.2	45.9	15.9	<b>13.9</b>	31.1	12.6	30.5
	SGC		17.5	75.4	25.8	<b>6.7</b>	15.3	53.8	42.4	11.2	0.0	33.4	11.8	26.7
	EdgeNet		<b>23.6</b>	<b>95.0</b>	28.6	<b>12.6</b>	13.1	<b>57.7</b>	<b>51.1</b>	16.4	9.6	<b>37.5</b>	13.4	32.6
Stanford 2D-3D-S	<b>Ours</b>	full (360°)	15.6	92.8	<b>50.6</b>	6.6	<b>26.7</b>	-	35.4	<b>33.6</b>	-	32.2	<b>15.4</b>	<b>34.3</b>